

Effects of different climatic conditions on soil water storage patterns

Annelie Ehrhardt^{1,2}, Jannis Groh^{1,3,4}, Horst H. Gerke⁵

5 ¹ Leibniz Centre for Agricultural Landscape Research (ZALF), Research Area 1 "Landscape Functioning", Working group
"Isotope Biogeochemistry and Gas Fluxes", Eberswalder Straße 84, 15374 Müncheberg, Germany

² TU Bergakademie Freiberg, Institute for Drilling Technology and Fluid Mining, Agricolastraße 22, 09599 Freiberg, Germany

10 ³University of Bonn, Institute of Crop Science and Resource Conservation (INRES) -- Soil Science and Soil Ecology, Nußallee
13, 53115 Bonn, Germany

⁴Institute of Bio- and Geoscience IBG-3: Agrosphere, Forschungszentrum Jülich GmbH, Jülich, 52425, Germany

⁵Leibniz Centre for Agricultural Landscape Research (ZALF), Research Area 1 "Landscape Functioning", Working group
"Silicon Biogeochemistry", Eberswalder Straße 84, 15374 Müncheberg, Germany

15 *Correspondence to:* Annelie Ehrhardt (annelie.ehrhardt1@mineral.tu-freiberg.de)

Abstract.

The soil water storage (SWS) defines crop productivity of a soil and varies under different climatic conditions.

20 Pattern identification and quantification of these variations in SWS remains difficult due to the non-linear behaviour of SWS changes over time. Wavelet analysis (WA) provides a tool to efficiently visualize and quantify these patterns by transferring the time series from time into frequency-domain.

We applied WA to an eight-year time series of SWS, precipitation (P), and actual evapotranspiration (ET_a) in similar soils of lysimeters in a colder and drier location and a warmer and wetter location within Germany. Correlations between SWS, P, and ET_a at these sites might reveal the influence of altered climatic conditions but also of subsequent wet and dry years on SWS changes.

25 We found that wet and dry years exerted influence on SWS changes by leading to faster or slower response times of SWS changes to precipitation in respect to normal years. The observed disruption of annual patterns in the wavelet spectra of both sites was possibly caused by extreme events. Extreme precipitation events were visible in SWS and P wavelet spectra. Time shifts in correlations between ET_a and SWS became smaller at the wetter and warmer site over time in comparison to the cooler and drier site where they stayed constant. This could be attributed to an earlier onset of the vegetation period over the years and thus to an earlier ET_a peak every year. This reflects the impact of different climatic conditions on soil water budget parameters.

1 Introduction

35 The soil water storage capacity (SWSC) is defined as the amount of water stored within the plant root accessible upper part of the vadose zone (e.g., Kutilek & Nielsen, 1994). Both, the SWSC and the process of soil water storage (SWS) within the root zone are important for defining the crop productivity (e.g., Stocker et al., 2023). The SWS in the vadose zone, i.e., the region between surface and groundwater table, has furthermore been considered a key for understanding ecohydrological interactions within the soil-water-atmosphere continuum (Vereecken et al., 2022).

40 The SWS is a dynamic component of the soil or ecosystem water balance equation and varies within the usually assumed constant SWSC. The SWS has been determined in the field by vertically integrating the soil water content obtained by point measurements using either soil moisture sensors or soil samples (gravimetric method) (e.g., Kutilek & Nielsen, 1994). Observation methods for quantification of the soil water balance for larger soil volumes include lysimeters, hydro-gravimeters, or cosmic-ray neutron sensor

45 networks (Heistermann et al., 2022). The SWS increases due to infiltration by rainfall, snowfall, irrigation, non-rainfall events (e.g., Groh et al., 2018), or upward-directed water movement from deeper soil layer or groundwater and lateral subsurface flow at hillslopes (e.g., Rieckh et al., 2014). The SWS decreases due to actual evapotranspiration (ET_a), lateral outflow, or vertical drainage. Annual changes in SWS have been used to quantify impacts of climate variability on plant growth and crop production (He
50 & Wang, 2019) or to analyze the susceptibility of soils towards floods and droughts (Shah & Mishra, 2021). The analysis of SWS changes was used to explain effects soil moisture variability on nutrient (Li et al., 2010; Shen et al., 2022) or carbon cycling (Lal, 2019) and ET_a in different land-use systems (Yang et al., 2016; Rahmati et al., 2020). The SWS depends on soil texture (e.g., Tafasca et al., 2020), soil structure (e.g., Rabot et al., 2018), organic carbon content (e.g., Hu et al., 2017), and vegetation properties
55 (Trautmann et al., 2022). Recent studies have shown that reoccurring drought years since 2015 have left severe deficits in the total water storage of catchments (Laaha et al., 2017) and continents (Boergens et al., 2020) that are unprecedented in the past 2110 years (Büntgen et al., 2021). Groh et al. (2020a) found that droughts can have an impact on the long-term SWS. The observation showed that SWS declined after a drought in 2015 and remained depleted until the end of the observation period, which implies long-term
60 effects of droughts (e.g., on the SWSC) and more importantly, the carry-over of the drought from one growing season to the next one. However, the SWS dynamics and their feedback to climate systems have been considered difficult to observe and comprehend (Vereecken et al.; 2022, Groh et al., 2020a; Herbrich & Gerke, 2017).

A common concept is that the SWS dynamics in the northern temperate climate zones have a dominant
65 annual cycle (Stahl & McColl, 2022) with the decrease during the growing period ($ET_a > P$) and the increase during the non-growing winter period ($P > ET_a$). In the longer term, the SWS approaches a soil- and site-specific mean value, which is usually defined according to the situation in the late spring (Groh et al., 2020a) just before the beginning of the growing period. The soil moisture conditions at this time of the year can be assumed to be optimally rewetted and in hydrostatic equilibrium. Water balance
70 calculations are mostly assuming that the SWS approaches approximately the same value at field capacity in late spring and that the SWSC remains constant.

Of course, the SWS patterns may differ within the annual cycles for agricultural crops and natural vegetation (Jia et al., 2013). Longer-term changes in SWS patterns and SWSC can be expected when the soil properties are changing, which has been reported from situations of soil degradation and amelioration, 75 changes in land use and soil management (e.g., Palese et al., 2014; Yu et al., 2015). However, the effects of changing climatic conditions on temporal patterns in SWS time series have not been widely reported. Identification of such patterns might help to elucidate the impact of climate change on SWS as an important component of the ecosystem water balance. Robinson et al. (2016) demonstrated a drought-induced alteration of soil hydraulic properties and a decrease in SWS, but only indirectly using soil 80 moisture observations that are not representative for the effective root zone but rather a small fraction of the soil. This lack of studies results from methodical difficulties in determining dynamic changes because of the complex effects that account for changes in SWS at shorter and longer time scales (Chen et al., 2023).

To analyse these dynamics and derive reoccurring patterns in time series of SWS, a variety of methods 85 including principal component analysis, empirical orthogonal functions, wavelet transform, unsupervised learning like self-organizing maps, and empirical mode decomposition have been applied (Vereecken et al., 2016). However, these approaches do not allow to localize these patterns in time, and, in particular, not to determine annual or daily cycles within a signal or timeseries over the entire period or if these patterns are interrupted in time as it could be done with a wavelet analysis (WA). The WA provides such 90 a tool by decomposing a time series into several components, each accounting for a certain frequency band by comparing the signal with a set of wavelet functions of known frequency similar to Fourier transform that uses a set of sinusoidal functions. However, since the wavelet function has zero mean, it is localized in time (Farge, 1992).. Thus, the dominant frequencies of a time series can be derived with WA for each moment in time. In contrast, Fourier analysis calculates only the dominant frequency across the 95 entire time series (Torrence and Compo, 1998). In addition, it may be important to find correlations between two time series, which often consist of non-stationary datasets (Ritter et al., 2009). The wavelet coherency analysis (WCA) can reveal the similarity of two signals that might have been overlooked by traditional correlation analysis (Grinsted et al., 2004). For example, if two time series contain similar

frequencies but are only shifted in time against each other, Pearson correlation indicates only little
100 similarity between the signals in contrast to WCA (Bravo et al., 2020).

Wavelet coherence analysis has been applied to reveal different temporal correlations between matric
potential and precipitation for grassland and cropland (Yang et al., 2016). Liu et al (2017) showed that
difference in water uptake strategies between grassland and woodland was manifested in a decreasing
105 correlation between soil moisture and precipitation. Graf et al. (2014) investigated the spatiotemporal
relations in a forested catchment between water budget components and soil water content using the WCA
to identify the main source of uncertainty when closing the water balance at smaller time scales (daily,
weekly). Using WCA it was not only possible to derive correlations across different scales from non-
linear SWC or ET_a time series but also to determine the temporal shifts in the correlation patterns (e.g.,
Rahmati et al., 2020). To identify differences in temporal onset of soil water movement between a
110 lysimeter and a arable field soil, indicating possible occurrence of lateral subsurface flow, Ehrhardt et al.
(2021) applied WCA to soil moisture time series'. A faster SWC increase in the field soil in comparison
to that of the lysimeter was attributed to water entering the field soil laterally from higher terrain positions.
Ding et al. (2013) showed that pulses of irrigation water, changed the time shift between ET_a and SWC
at daily scale thereby demonstrating that irrigation can control the temporal variability of ET_a .

115 As an extension of WCA, multiple WCA (MWC) and partial WCA (PWC) have been developed (Hu &
Si, 2016, 2021). The MWC allows correlations with three or more variables as demonstrated for the
influence of meteorological factors on streamflow generation (Su et al., 2019) or soil physical parameters
on soil water content (Hu et al., 2017). The PWC can be applied when in bivariate relationships both
variables are dependent on each other; as for example, to determine precipitation amount and duration as
120 controlling factors of groundwater flow in humid and arid areas (Gu et al., 2022).

When analysing the effect of climate variability on SWS, it is plausible to compare time series of similar
soils under different climatic conditions (i.e., space-for-time substitution approach, e.g., Groh et al.,
2020a). If deviations in soil type and crop rotation can be excluded, deviations in SWS patterns between
the two places must be attributed to different climatic conditions. The hypothesis is that if there are no
125 differences in SWS patterns between the two sites, climatic conditions do not affect SWS. However, as
the soil develops differently under each local climate, the same soil can hardly be found under a different

climate. The situation can only be created experimentally. Within the TERENO-SOILCan lysimeter-network (TERrestrial ENvironmental Observatories; Pütz et al., 2016), lysimeters extracted (monolithically) from different land use types (natural and managed grassland, arable land) and soil types
130 have been transferred according to a modified space-for-time approach to sites with differing climatic conditions. This setup allows to evaluate the impact of altered climatic conditions on agricultural ecosystems (Pütz et al., 2016) and to quantify changes in the soil water cycle and crop production due to climate variability. In previous studies, the soil water balance components of the lysimeter at the original location have been compared with those of the transferred lysimeter to define the impact of different
135 climatic and management conditions on nitrogen leaching (Fu et al., 2017), to evaluate precipitation measurement methods (Schnepper et al., 2023), and to improve the modelling of hydrological processes and ecosystem productivity of the same soil but under different climatic conditions for arable-land and grassland ecosystems (Jarvis et al., 2022, Groh et al., 2022). Rahmati et al. (2020) demonstrated that due to increasing dryness, the SWS is stronger controlled by ET_a for a grassland soil. They explained declining
140 phase shifts between ET_a and SWS at the annual scale over a 7-years period with increasing dryness and suggested that this might also be the case for cropland soil.

Still, long-term studies on trend analysis and pattern detection in SWS time series to derive the effect of changing climate on SWS components in cropland are limited and restricted to larger scales like satellite observations (e.g., GRACE-REC, Humphrey & Gudmundsson, 2019). Agboma and Itensifu (2020)
145 observed increasing periodicity in SWS changes with increasing soil depth that might be relevant for seasonal soil moisture regime forecasting. They concluded that such studies are still missing for cultivated cropland because most monitoring sites for SWS observation are in grassland. Chen et al. (2023) identified different governing parameters on SWS stability in winter and summer highlighting the need for these analyses on long-term data to derive impacts of extreme climate change on hydrological
150 variables.

To gain more insights on SWS patterns evolving for the same soil under different climatic conditions in cropland for an eight-year observation period (2014 until 2021), we employ WCA to compare SWS time series of a soil at its original location to SWS of this soil transferred to a wetter and warmer climate. We want to analyse, if SWS patterns can be assumed to be independent of the site-specific climatic conditions

155 and thus be assumed to be entirely dependent on the soil conditions. We hypothesize that there is no
variation in SWS of the similarly managed arable soils at the two sites if SWS patterns are independent
of the climatic conditions. Our objectives are (i) to detect temporal patterns in SWS changes (SWS) of
the same soil under two different climatic conditions (drier and colder vs. wetter and warmer) with WA
and (ii) to visualize how other soil water balance components (precipitation P, ET_a , net drainage) are
160 affected or affect the SWS under different climatic conditions. We expect a quantitative temporal off-set
between daily, seasonal, and annual changes in the components of the soil water balance and effects on
SWS patterns, changing from those of a period with wet climatic conditions (2015-2017) to those in
subsequent dry years (2018-2020) due to carry-over effects.

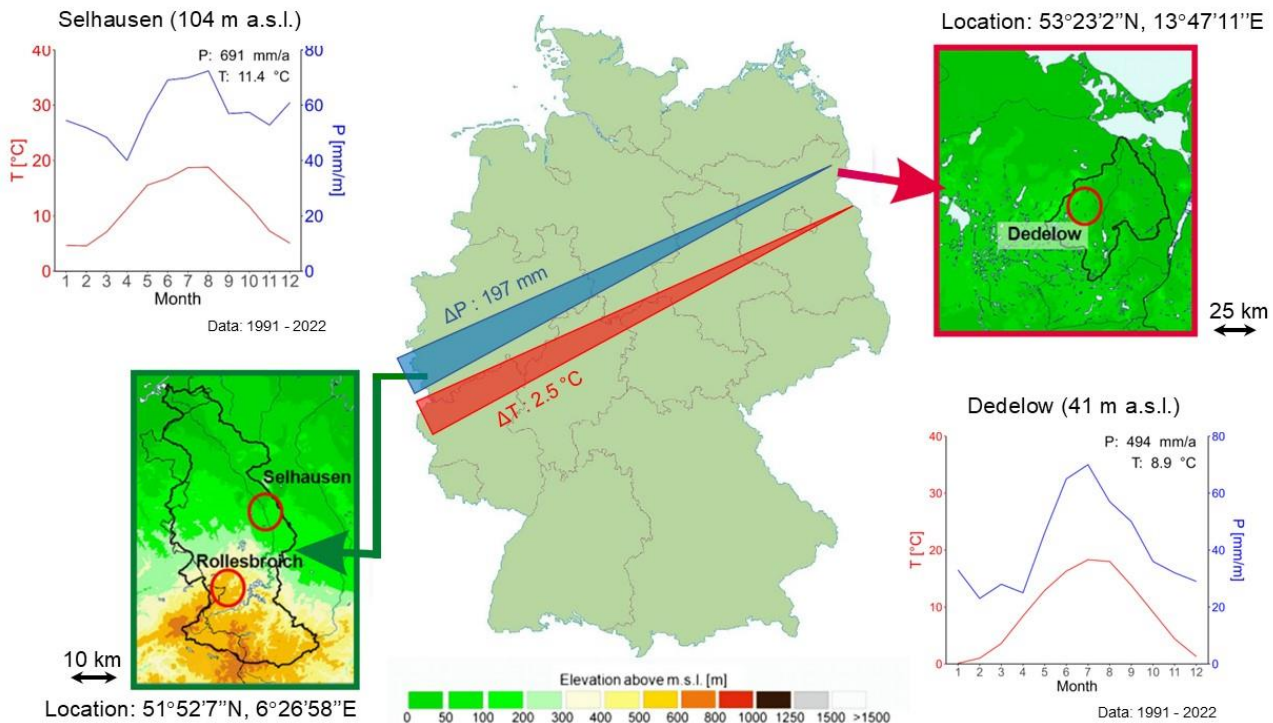
2 Materials and Methods

165 2.1 Site description

The study areas are located in Selhausen (51°52'7''N, 6°26'58''E) and Dedelow (53°23'2''N,
13°47'11''E) (Fig. 1). A total of nine high-precision weighing lysimeters (precision: 10 g, METER
Group) were filled with intact eroded Luvisol soil monoliths in Dedelow. Three out of nine lysimeters
were installed in Dedelow and three were transferred to Selhausen, and Bad Lauchstädt each to expose
170 the extracted soil to different climate regimes. For the purposes of this study, we will only address the
lysimeter measurements at the Dedelow and Selhausen sites. The transfer from Dedelow to Selhausen
corresponds to an increase in annual precipitation sum of 112 mm and an increase in average annual
temperature of 1.6 °C throughout the study period (2014-2021) (Luecke et al., 2024). Thus, within these
eight years, the lysimeters from Dedelow were exposed to slightly wetter and warmer weather conditions
175 caused by a more oceanic climate in Selhausen as compared the more continental one in Dedelow. Also,
considering the two sites with the different climatic conditions, the weather was characterized by extreme
rainfall events (2017), relatively wet (2017, 2021) and dry (2018) periods within the observation period.
Compared with the longer-term periods, these extremes seem to be exceptional.

The experimental set-up is part of the TERENO-SOILCan lysimeter network (Pütz et al., 2016). The
180 lysimeters are 1.5 m deep and have a surface area of 1 m². The soil water dynamics at the lysimeter bottom

were adjusted to field conditions by a bi-directional pumping control system that adjusts measured pressure head at the bottom of the lysimeter to measured pressure head in a similar depth in the field. During drainage periods water from the lysimeter was collected via a suction rake at the bottom of the lysimeter in a weighable seepage tank (precision: 1 g). In periods with an upward directed water flow from capillary rise, the water was pumped back into the lysimeter from the seepage tank. For more details on the lysimeter set-up and equipment refer to Groh et al. (2020a, b). The lysimeters were embedded within larger fields in Selhausen (0.025 ha) and Dedelow (2.3 ha), where the plant management in the lysimeter and the field was identical during the observation period.



190 **Figure 1: Location of the sites Dedelow and Selhausen in Germany with climatic diagrams comparing the 30-years average values**
 of monthly precipitation (P, mm/m) and average monthly temperature (T, °C). The gradients in annual mean precipitation (ΔP) and
 mean annual temperature (ΔT) between the site Selhausen (left, located in the west of Germany) and Dedelow (right, located in the
 195 northeast of Germany) for the period 1991 – 2022 is indicated by the red and blue elongated triangles. Dedelow receives on average
 197 mm per year less P than Selhausen and on the annual average temperature is about 2.5 °C less than at the site in western
 Germany. Elevation scale refers to the topographic maps.

The climate in Dedelow with an average annual P sum of 494 mm and an average annual temperature of 8.9 °C (1991-2022) is more continental than the climate in Selhausen with an average annual P sum of 691 mm and an average annual temperature of 11.4 °C (1991-2022). The P distribution is unimodal at

both sites with a peak in summer. Average monthly temperatures in Dedelow experience a minimum in
 200 January with 0.1 °C and a maximum in July with 18.3 °C, whereas temperatures in Selhausen vary
 between 4.5 °C in February and 18.8 °C in August indicating a slightly smaller annual temperature
 amplitude between winter and summer for Selhausen. Average monthly temperatures and P (Fig. 1) were
 obtained from automated weather stations in Dedelow (SYNMET/LOG, LAMBRECHT meteo GmbH)
 and Selhausen (weather station of the Forschungszentrum Jülich; the data are available at:
 205 <https://teodoor.icg.kfa-juelich.de/ibg3searchportal2/index.jsp>, station ID ru_k_001). During the
 observation period the Selhausen was subject to a slightly lower wind speed (0.3 m s⁻¹) than Dedelow.
 All soils are Haplic Luvisols. The soil monoliths were extracted at a midslope positions along a 20 m
 transect of an agricultural field site as close as possible to each other (~3 m apart; Herbrich & Gerke,
 2017). The texture of the Ap-, E+Bt-, and eCv-horizons was described as loamy sand. The clay content
 210 in the Bt-horizon is slightly higher than in the other horizons indicating a more loamy texture (Tab. 1).
 A detailed description of horizons of the single lysimeters can be found in the supplement of Groh et al.
 (2022). The variation between the different lysimeters is relatively small as is the variation in horizon
 depth between the lysimeters, so only the mean values between the different lysimeter soils are reported
 in Tab. 1.

215 **Table 1: Horizon depths, soil bulk density (ρ_b), porosity (ϵ) and texture (sand: 2.0 to 0.063 mm; silt: 0.063 to 0.002 mm; clay: < 0.002 mm) for the lysimeter Dd_1 located in Dedelow. The other lysimeters differed only in the thickness of the diagnostic horizons below the Ap-horizons. Data are from Herbrich & Gerke (2017). Supporting information (e.g., soil hydraulic properties): see also Groh et al. (2022)**

Horizon*	Depth [cm]	ρ_b [g cm ⁻³]	ϵ [cm ³ cm ⁻³]	Sand [g kg ⁻¹]	Silt [g kg ⁻¹]	Clay [g kg ⁻¹]
Ap	0-30	1.53	0.42	538	305	157
E+Bt	30-42	1.65	0.38	510	341	149
Bt	42-80	1.52	0.43	507	299	194
eCv	80-150	1.69	0.36	589	293	118

*Horizons named according to FAO classification (IUSS Working Group WRB, 2015)

220 The field crops varied each year (Tab. 2) but were similar for Dedelow and Selhausen despite for 2014,
 when oat was grown in Selhausen and Persian clover in Dedelow. However, as the different crops were
 planted at the beginning rather than in the middle of the time period, the impact was expected to be
 minimal. In addition, in 2015/2016 winter wheat was planted in Dedelow instead of winter barley was
 planted in Dedelow. As both crops are winter cereals, only minor deviances are expected.

225 **Table 2: Field crops, dates of sowing and harvest (format [dd-mm-yyyy]), duration of vegetation period in days (Veg. per.) and amount of precipitation (P) in mm during the vegetation period for the lysimeters in Selhausen and Dedelow (average values from three repetitions)**

Year	Selhausen					Dedelow				
	Crop	Sowing	Harvest	Veg per. [d]	P [m m]	Crop	Sowing	Harvest	Veg per. [d]	P [m m]
2014	Oat	05-03-2014	03-06-2014	90	141	Persian clover	04-03-2014	24-07-2014	142	247
2015	Winter wheat	15-10-2014	21-07-2015	279	501	Winter wheat	17-09-2014	23-07-2015	309	443
2016	Winter barley	07-10-2015	08-07-2016	275	632	Winter wheat	02-10-2015	27-07-2016	299	447
2017	Winter rye	11-10-2016	21-07-2017	283	453	Winter rye	06-10-2016	02-08-2017	300	732
2018						Winter barley	20-10-2017	10-04-2018	173	313
	Oat	15-03-2018	24-07-2018	131	176	Oat	11-04-2018	27-07-2018	107	101
2019	Winter Wheat	05-11-2018	24-07-2019	261	441	Winter wheat	09-10-2018	25-07-2019	289	421
2020	Winter barley	30-09-2019	07-07-2020	281	553	Winter barley	26-09-2019	02-07-2020	280	381
2021	Winter rye	20-10-2020	04-08-2021	288	643	Winter rye	06-10-2020	26-07-2021	293	578

2.2 Soil water storage, actual evapotranspiration and precipitation data

230 The long-term weather observations (1991-2022) were obtained from close-by stations at Selhausen and Dedelow. The lysimeters were established in 2010 and the P and ET_a data were obtained from mass changes of the lysimeters (Schrader et al, 2013, Schneider et al., 2021). Weight changes (i.e., the changes in mass) of the lysimeters were collected in 1-min resolution and aggregated to hourly values. The raw data were checked manually as well as automatically according to Pütz et al. (2016) and Schneider et al.

235 (2021). To further reduce the impact of noise on the determination of ET_a and P data, the adaptive window and threshold filter (AWAT, Peters et al., 2017) was applied. Missing data were gap-filled on aggregated hourly basis within the post-processing scheme. In a first step, a linear regression model was applied that was using the mean value of ET_a and P calculated from values of all available lysimeters with the corresponding soil. In a second step, remaining gaps were gap-filled by a linear regression model that was

240 using reference data from a rain gauge or reference evapotranspiration (grass) according to the Penman

Monteith method (Allen et al., 1998). A detailed comparison between P data from lysimeter and standard rain gauges can be found in Schnepper et al. (2023).

Values of hourly soil water storage changes ΔSWS [mm h^{-1}] were calculated according to:

$$\Delta SWS = P - ET_a - Q_{net} \quad (1)$$

245 where Q_{net} refers here to the hourly sum of net water flux [mm h^{-1}] across the lysimeter bottom ($Q_{net} > 0$: drainage, $Q_{net} < 0$: capillary rise).

The cumulative change in total soil water storage, SWS_t [mm], from the value at the beginning of the measurements, SWS_0 [mm], was obtained by integrating (i.e., which is here identical with summing hourly values) ΔSWS as:

$$250 \quad SWS_t = SWS_0 + \sum_{i=1}^N \Delta SWS_i \Delta t_i \quad (2)$$

for every hour, i , till the end ($N = 70080$ h) and for each of the lysimeters.

For the following analysis (WA and WCA) the mean between three replicate lysimeters was calculated for each hour and component of the soil water balance.

2.3 Wavelet analysis and wavelet coherence analysis

255 The complex Morlet wavelet (wavenumber $k_0 = 6$) was selected as a mother wavelet for the continuous wavelet transform of the time series. The Morlet wavelet is well suited for the analysis of environmental signal due to its good balance of time and frequency resolution (Grinsted et al., 2004). Also, due to its complex nature amplitude and frequency of the signal can be reproduced (Torrence & Compo, 1998). As a background spectrum, a first-order autoregressive process (red noise) was chosen to test the significance
260 of the wavelet spectra. For the visualization of the wavelet spectra and the wavelet coherence spectra, a significance level of 10 % against this background spectrum was applied. 300 Monte Carlo simulations were conducted to find the regions of significant periodicities. For smoothing of the wavelet spectra, a Blackman window was selected to amplify the significance within the single wavelet spectra (Torrence and Compo, 1998). For the time series no detrending was performed. Calculation of the wavelet plots and
265 wavelet coherence plots was performed according to Torrence & Webster (1999) and executed in the R software v. 3.6.2 (R Core team, 2019) with the package WaveletComp (Roesch & Schmidbauer, 2018). Variables used for the WCA were the SWS, P, ET_a , and Q_{net} in Dedelow and Selhausen. For correlations

between the two locations the data set from Dedelow was the base signal and data from Selhausen as the second signal. P and ET_a were used as the base signals for correlations between P and SWS and between
270 ET_a and SWS.

WCA does not only derive times and scales of correlation between two signals but also how the periodic fluctuations of the time series are shifted in time against each other. General trends in phase shifts are indicated by the arrows within the significant parts of wavelet coherence spectra. They can be quantified by analysing the phase angle derived from the imaginary and real part of the cross-wavelet spectrum (Si,
275 2008). The phase angle is calculated in radians in the range from $-\pi$ to $+\pi$. Depending on the scale of interest, π corresponds to a time shift of 12 h at the daily (24 h) scale and to 4380 h at the annual (8760 h) scale.

For more details on the theoretical background of wavelet and wavelet coherence analysis refer to Si & Zeleke (2005) and Grinsted et al. (2004).

280 **3 Results and Discussion**

3.1 Comparison of SWS, ET_a and P under different climatic conditions

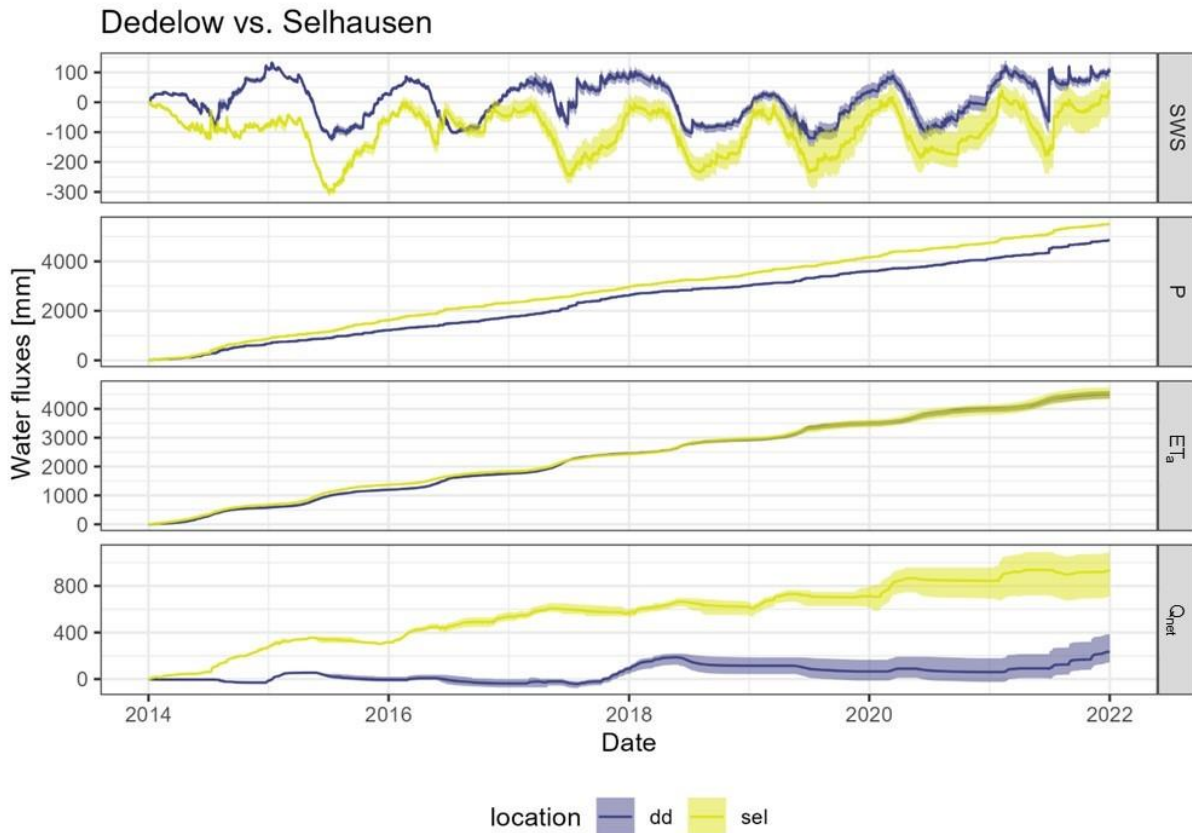
Throughout the observation period (2014-2021), the SWS values ranged from -100 to +100 mm relative to the initial value of SWS_0 at the beginning of the period for Dedelow and between -300 and +25 mm for Selhausen (Fig. 2). The annual fluctuations in SWS were more pronounced in Selhausen (wetter and
285 warmer climate) as compared to Dedelow (drier and colder climate). For Selhausen, the year 2015 brought an extreme decline in SWS (-300 mm) due to a drought that spread not only to the local region but to large parts of Europe (Ionita et al., 2017). For Dedelow, the years 2018 and 2019, which included the extreme drought in 2018 (Büntgen et al., 2021), were characterized by extremely dry conditions, which led to a decrease in SWS and an early ripening of the oat crop (Groh et al., 2019).

290 Wetter years with a more than average P amount were 2014 (+37% above average) and 2017 (+77%) for Dedelow and 2014 (+26%) for Selhausen (Table A1). From 2014 to 2021, the total amount of P per year decreased with minimum values of 400 mm a^{-1} in 2018 for Dedelow and 534 mm a^{-1} in 2018 for Selhausen. Note that the average value of P (2014-2021) was significantly higher than the P for the

295 respective reference period (1991-2022) determined by standard rainfall gauges, which underestimate P
as compared to the more realistic lysimeter P data (Schnepper et al., 2023). In addition, P amounts
determined with lysimeters include water from non-rainfall events (i.e., dew formation), which
contributed 7.2 % on the annual scale of total P for the period 2015-2018, at least for Selhausen and the
nearby Eifel region (Forstner et al., 2021, Groh et al., 2020b).

300 Note the extreme increase in SWS in both locations in July 2021 that was caused by an extreme
precipitation event with up to 174 mm in Dedelow and 103 mm in Selhausen within two days causing
major flooding within the Eifel-Ardennes Mountains in Germany (Lehmkuhl et al., 2022).

Daily ET_a rates experienced annual cycles with a maximum in 2015 for Selhausen (691 mm a^{-1}) and in
2017 for Dedelow (700 mm a^{-1}), which was 22 % and 24 % more than the average annual ET_a value at
the corresponding site (Table A1). The bottom drainage of the lysimeters was much smaller in Dedelow
305 than in Selhausen (Fig. 2) corresponding to the drier climatic conditions at the more continental
experimental site.

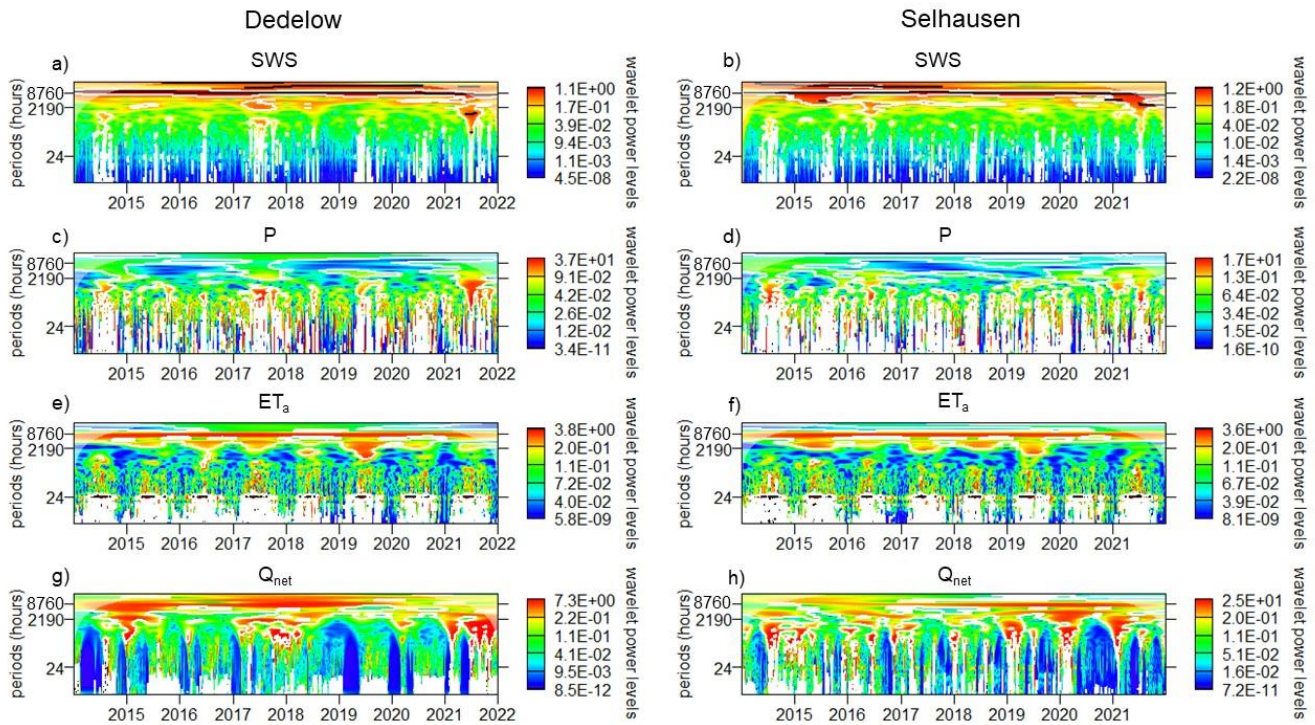


310 **Figure 2: Hourly soil water storage change (SWS) and cumulative sum of precipitation (P), actual evapotranspiration (ET_a) and bottom flux (up- and downwards, Q_{net}) of the lysimeters since 01-01-2014 in Dedelow (dd) and Selhausen (sel). The shaded areas represent the cumulative minimum and maximum values of the hourly data derived from the three lysimeters at each of the two sites.**

315 These annual variations in SWS and ET_a observed in the time series were reflected in the wavelet spectra (Fig. 3). For SWS both wavelet spectra in Selhausen and Dedelow showed significant periodicities (area within the white edging) at the annual scale (period = 8760 h) over the entire observation period (Fig. 3 a, b). Such annual patterns in SWS changes have been also found by Liu et al. (2020) for the Shale Hills catchment in Pennsylvania; USA. They related these fluctuations to seasonal variations due to water consumption by plants (transpiration) and soil evaporation. We assume that in our study also the crop transpiration is the main reason for the observed seasonal fluctuations. At the daily scale (period = 24 h), a diurnal variation throughout the vegetation period was vaguely perceptible as indicated by the bright

320 sky blue band at the 24 h-scale (Fig. 3 a, b). This diurnal fluctuation was however not significant against the red-noise background spectrum.

The influence of wet and dry years was visible in the wavelet spectra of the SWS changes (Fig. 3 a, b): At scales higher than the annual scale, significant periodicities were found for Dedelow between 2017 and 2021 and for Selhausen between 2015 and 2021 at the two-year scale. Significant periodicities in
325 SWS changes extended towards smaller scales (semi-annual to monthly) in Dedelow in 2015, 2017 and 2021 that correspond to years with more than average P (Table A1) that is also visible in the wavelet spectra of P (Fig. 3 c). For Selhausen, significant periodicities were found at smaller scales (e.g. monthly) in the years 2014 and 2021 corresponding to years with an increased P amount (Table A1) like in Dedelow. In the wavelet spectra of P for Selhausen, periodicities extending to monthly scales were found
330 also for the year 2016 (Fig. 3 d) that has been characterized with an extremely low ET_a (-18% than average year). Also, in 2016 Selhausen received 200 mm more P throughout the vegetation period (Tab. 2), possibly explaining the differing SWS patterns in comparison to those for Dedelow.



335 **Figure 3: Wavelet spectra of the soil water storage change (SWS), P, ET_a and bottom drainage Q_{net} (up- and downward flux) of the lysimeters in Dedelow and Selhausen. Time is depicted on the x-axis and the y-axis denotes the periodicity in hours (24h = daily scale,**

8760 h = annual scale). The colour indicates the wavelet power level that shows the similarity of the frequency of the wavelet with the frequency of the time series at the given scale and at the point in time. Areas in the wavelet spectrum that deviate significantly from the red noise background spectrum (significance level = 10 %) are surrounded by the white edging. Since at smaller scales the white rim (indicating significant areas in the wavelet plots) is rather omnipresent, the average significant periodicities are indicated by black lines (e.g., panel f). A logarithmic scale for the wavelet power levels was chosen to amplify differences in wavelet coefficients between different parts of the spectra visually. The shaded area at the edge of the plot at higher scales is called the cone of influence. Here, edge effects due to the padding of the time series with zeroes at the beginning and the end might influence the appearance of the wavelet spectrum and thus should be interpreted with caution.

As already shown for Dedelow, the years 2014 and 2021 with increased P were also visible in the significant areas of the wavelet spectrum for Selhausen (Fig. 3 d).

Extreme drought events and vegetation periods are reflected in the wavelet spectra for ET_a in Dedelow and Selhausen that showed distinct annual cycles (Fig. 3 e, f). Also, the periodicities at the daily scale were significant throughout the vegetation period at both sites indicating the influence of vegetation on increased ET_a . In 2019 the spectra of both sites showed significant periodicities extending to smaller scales corresponding to a year with extreme drought in Germany (Boeing et al., 2022).

The wavelet spectra of Q_{net} of the lysimeters showed a distinct annual fluctuation in Dedelow from 2014 to 2019, whereas in Selhausen this annual cycle occurred between 2016 and 2021 (Fig. 3 g, h). At the drier site in Dedelow, the years with more P were well distinguishable by significant periodicities extending towards smaller scales (Fig. 3 g). In Selhausen these patterns were observed almost every year (Fig. 3 h).

The higher amplitude in the annual fluctuations of SWS in Selhausen (Fig. 2: SWS: 300 mm) in comparison to Dedelow (Fig. 2: SWS: 200 mm) was reflected in the global wavelet power that is obtained when averaging the wavelet coefficients of a time series over an entire scale (Fig. 4 a, d).

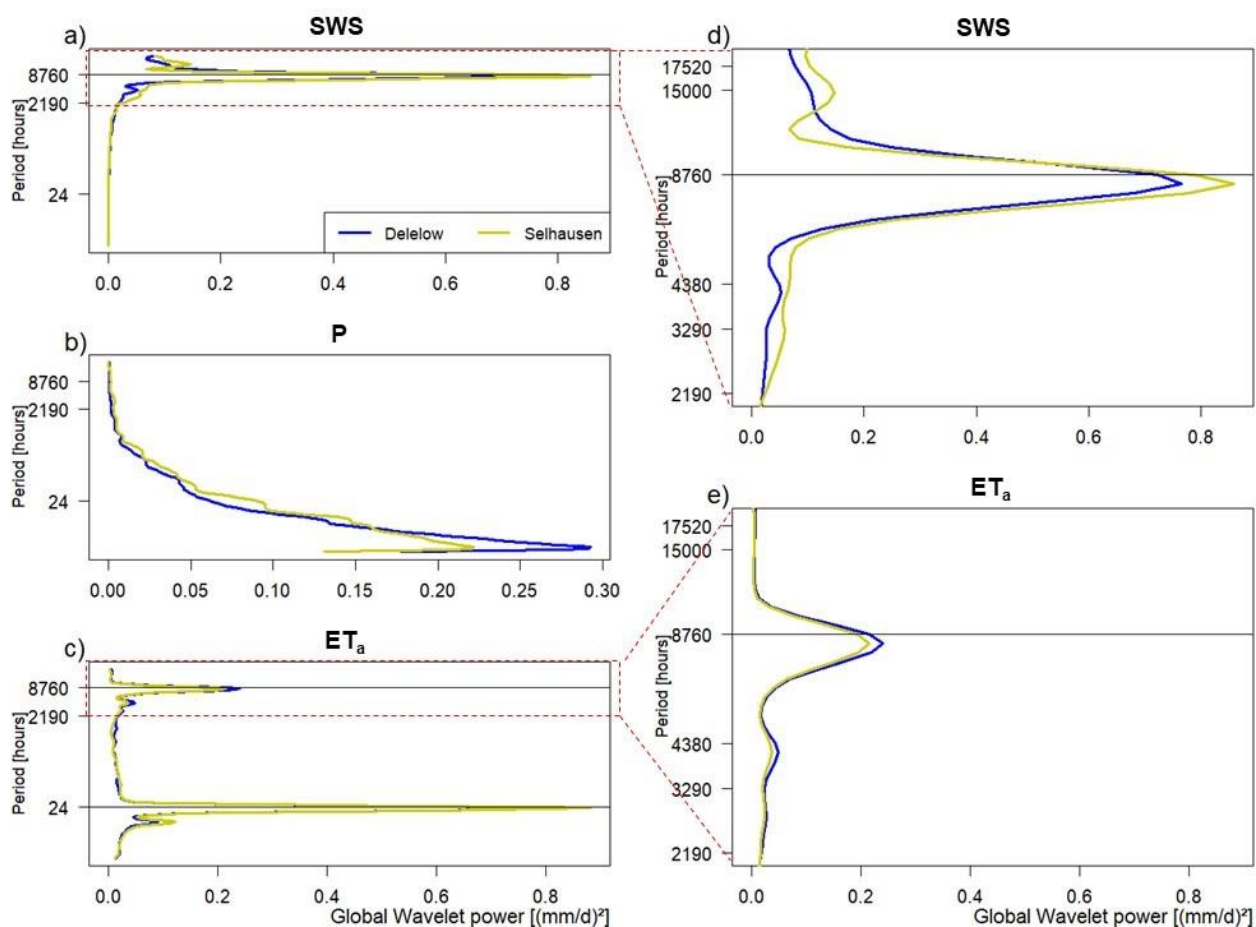


Figure 4: Global wavelet coefficients of soil water storage (a), precipitation (b), actual evapotranspiration (c) across different scales in Dedelow and Selhausen. (d) and (e) are close-ups of the SWS and ET_a at the annual scale, respectively.

This could be attributed to the higher annual P amount in Selhausen in contrast to Dedelow, especially since the ET_a was similar for both sites on average (Table A1). In contrast to Dedelow, a small peak around a period of approximately 16500 hours was found in Selhausen (Fig. 4 d) indicating a two-year cycle that was already found in the wavelet spectra (Fig. 3 b).

For P no annual pattern was found in the global wavelet spectra but at a periodicity of approximately 6 hours, a peak was observed in both spectra (Fig. 4 b). This peak was more pronounced for the drier site in Dedelow, however, the global wavelet power was much smaller in comparison to SWS and ET_a.

For ET_a strong peaks in the global wavelet spectra were found at the daily and at the annual scale (Fig. 4 c, e). Also, a small peak at a periodicity of around 4380 h was observed for ET_a responding to a

semi-annual cycle attributed to the length of the vegetation period. Note that the peaks in SWS changes and ET_a values around the annual scale were occurring slightly below a periodicity of 8760 h that corresponded to the exact number of hours per year. This could indicate a temporal shifting of the annual cycles, possibly caused by different climatic conditions. For example, Rahmati et al. (2023) showed that in Europe since 1981 the start of the vegetation period and the dry period was shifted towards earlier times in the year. Thus, the total difference in days between the start of the vegetation period of the preceding year and the following year decreases over time leading to a shift of annual cycles towards lower periodicities.

380 **3.2 Correlation and time shifts between soil water budget variables of both sites reflect dominant climatic patterns**

Correlating the SWS, P and ET_a fluctuations between Dedelow and Selhausen by WCA might reveal the effects of changing climatic conditions on the soil water budget that was not directly visible from the time series itself (e.g. Biswas & Si, 2011).

385 Carry-over effects of dry years are found in the WCA spectra when correlating SWS changes from the drier and colder site with those from the wetter and warmer site. The coherence plot of SWS between Dedelow and Selhausen revealed a highly significant correlation pattern at the annual scale, which is only interrupted in 2017 (Fig. 5 a). The year 2017 has been denoted as an extreme wet year in Dedelow with almost 77 % more P than average (1991-2022). On the two-year scale, significant correlations between
390 the two experimental sites were found from 2020 to 2021 with a positive phase shift indicating an earlier rewetting phase in Dedelow than in Selhausen (Fig. 5 b, i). This trend is opposite to the phase shifts found at the annual (Fig. 5 b, ii) and semi-annual scale (Fig. 5 b, iii). It could indicate the carry-over effect of SWS deficit from the previous drought year 2020 as already described by Groh et al. (2020a) for different soils at the experimental site in Bad Lauchstädt.

395

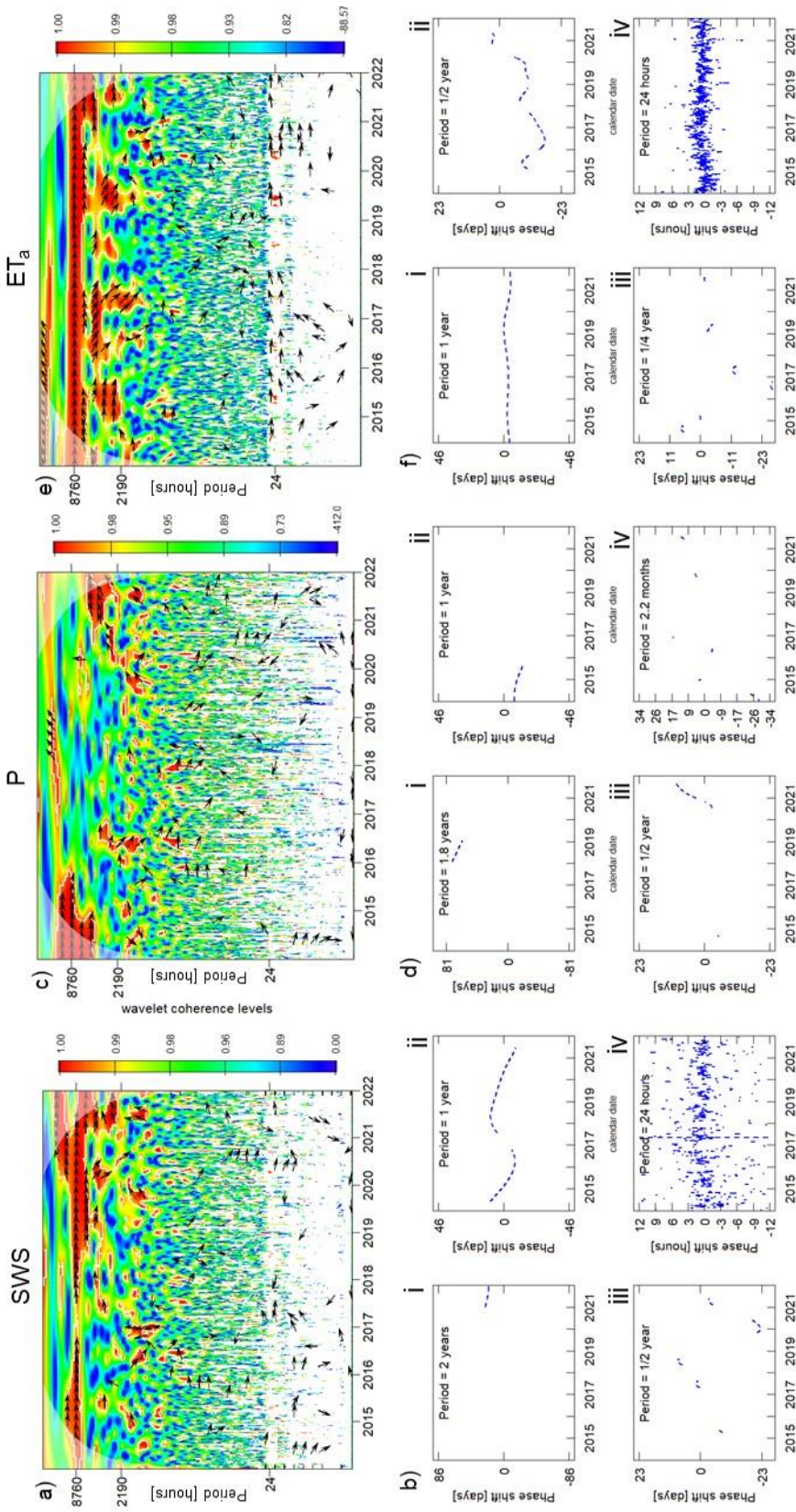


Figure 5: Wavelet coherence plots showing the correlation between Dedelow and Selhausen of SWS (a), precipitation (c) and actual evapotranspiration (e). For explanation of the plot layout refer to Fig. 3. The black arrows indicate the phase shift in the correlation of these variables between Dedelow and Selhausen. Arrows showing to the right indicate a perfect correlation without any shift in time. Arrows pointing upwards indicate a leading pattern for the plots in Dedelow whereas arrows pointing downwards show a leading pattern for Selhausen. These phase shifts can be expressed quantitatively in hours or days (b, d, f) for a given scale within in significant parts of the WCA spectrum. Negative and positive phase shifts correspond to a leading pattern for Dedelow and Selhausen, respectively.

Significant correlations extended towards smaller scales (semi-annual and quarterly scales) in spring 2015, autumn 2017 and 2018, winter 2019/2020 and spring 2021 possibly reflecting the influence of plant growth on SWS (Fig. 5a). In 2016 no correlations between the two sites were found that might be
400 attributed to the much smaller P amount throughout the vegetation period in Dedelow compared to Selhausen (Tab. 2).

The influence of wet and dry years was reflected in changing phase shifts between the two sites. No considerable temporal deviations in SWS changes at the annual scale were found between Dedelow and Selhausen in Fig. 5 a (arrows indicating phase shift). However, when directly plotting the phase shift from
405 the significant parts of the WCA spectrum, a slightly negative off-set was found until 2017 at the annual and semi-annual scale (Fig. 5 b) for the variable SWS change. This refers to an in general faster decrease in SWS in Selhausen than in Dedelow. In 2017 this trend was reverted into a positive phase shift showing a faster change in SWS in Dedelow than Selhausen, due to the exceptional high P during this year in Dedelow. After the drought year 2020, again negative phase shifts were observed at the annual and semi-
410 annual scale. Thus, wetter and drier years exerted influence on SWS changes by leading to faster or slower response times in SWS as compared to normal years.

At the daily scale significant correlations in SWS between the two sites were found throughout the entire observation period (Fig. 5 a) without any time shifts (Fig. 5 b, iv) indicating similar diurnal patterns at both sites.

415 Dominant climatic deviations in P input and in the onset between the drier and the wetter site were found when correlating the P time series of Dedelow and Selhausen. The P patterns showed significant correlations at the annual scale at the beginning of the observation period in 2014/2015 (Fig. 5 c). A slightly negative phase shift indicated a faster onset of P in Selhausen compared to Dedelow (Fig. 5 d, ii) that could be attributed to the west wind drift dominating the weather patterns in middle Europe. From
420 2018 to 2019 a two-year cycle was observed with a positive phase shift (Fig. 5 d, i). Likewise, changed patterns in the SWS could be attributed to carry-over-effects of low P in drought years. In 2021 a significant area in the WCA spectrum was found at the semi-annual scale with a positive phase shift of approximately twelve days (Fig. 5 d, iii) indicating a faster onset of P at the site Dedelow compared to Selhausen. This corresponds well to the temporal shift between the heavy P events at these two sites in

425 July 2021. In Dedelow 174 mm of P were recorded from June 30th to July 1st, 2023. Twelve days later
Selhausen received 103 mm of P from July 13th to July 14th, 2023. The time shift between the P events
was also found at the quarterly scale (Fig. 5 d, iv). This demonstrates the efficiency of WCA to derive
information about time shifts that cannot directly be conceived by regular time series analysis. These time
shifts in the P are most likely caused by deviations due to the different longitude of both locations and the
430 pattern is related to the European west wind drift (Hu et al., 2022).

The shift of the start of vegetation periods towards earlier times of the year over the observation period
could be deduced from the WCA spectra of ET_a . ET_a showed high correlations between Dedelow and
Selhausen at the annual scale over the entire period (Fig. 5 e). The correlations were well in phase
showing no time shift between the patterns of the two sites (Fig. 5 f). At the semi-annual scale significant
435 correlations occurred throughout the vegetation period (Fig. 5 f, ii). Between 2015 and 2020 the phase
shifts at the semi-annual scale were negative. Since ET_a was directly related to the plant development this
indicates a faster onset of the vegetation period in Selhausen than in Dedelow with delays of 5 to 15 days
as it is found from calculating the onset of the vegetation period from temperature data (Fig. 8). Only in
2021 this shift was inverted to a positive phase shift. As already indicated in the wavelet spectra
440 (Fig. 3 e,f) a highly significant correlation between ET_a in Dedelow and Selhausen was found at the daily
scale. The phase shift oscillated around zero hours (Fig. 5 f, iv) indicating similar diurnal patterns for the
two sites like it was found for the SWS changes (Fig. 5 b, iv).

For Q_{net} our analysis showed for the most years a clear shift between the sites indicating that the rewetting
of the same soil started at the wetter site Selhausen earlier in the non-growing season compared to the
445 drier site in Dedelow (Figure C1). Only for the very wet year 2017 a shift towards earlier rewetting in
Dedelow is visible. At smaller scales this is also visible for the extreme P event in 2021 where the P
occurred earlier in Dedelow than in Selhausen (Figure C2 and C3).

These results imply that climatic conditions indeed have distinct effects on SWS patterns, which are
especially found in extreme years. As the climate is about to become more extreme (e.g., as suggested by
450 Rahmstorf et al. (2024) due to a weakening of the gulf stream in northern Europe), these patterns might
persist over the years. Temporal changes in SWS that increase over winter time and decrease over summer
time may then affect crop production or the infiltration capacity of soils during extreme events.

3.3 Correlation and time shifts between soil water budget components at each site

The response time of the SWS to P input was deduced from the WCA spectra between P and SWS. The correlation between P and SWS in Dedelow and Selhausen occurred mainly at smaller scales corresponding to the return periods of P (Fig. 6 a, c). P and SWS had positive phase shifts across all scales (black arrows pointing upwards) showing that SWS changes were lagging behind P inputs. At a weekly scale this phase shift oscillates around 48 h for Dedelow and Selhausen indicating that approximately 2 days are needed to pass before changes caused by P lead to an increase in SWS (Fig. 6 b, d iv). Similar temporal delays (0.375 weeks) have been observed for correlations between P and the soil matric potential in cropland (Yang et al., 2016).

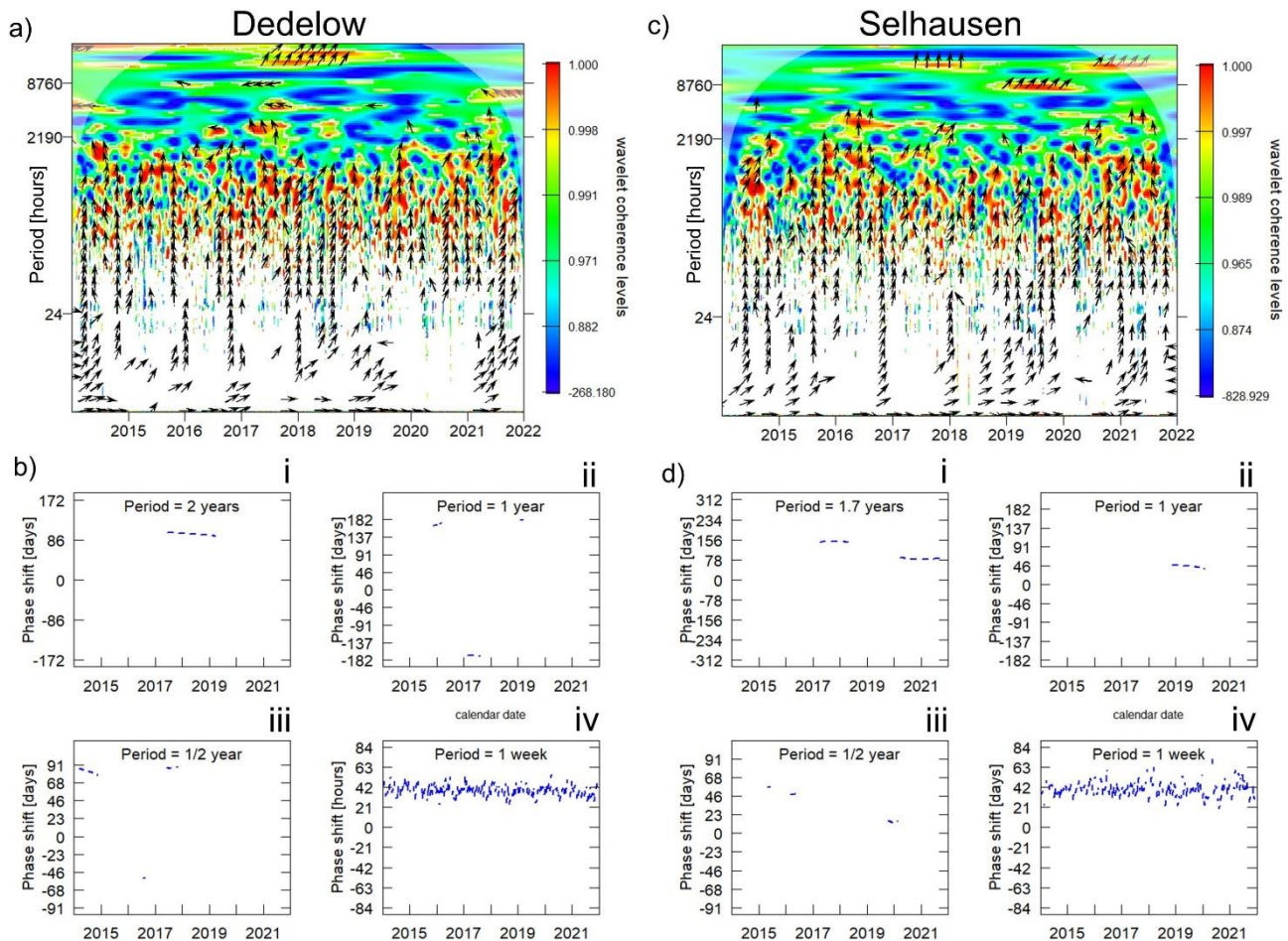


Figure 6: WCA between P and SWS in Dedelow (a) and Selhausen (c) and time shifts expressed in days and hours for selected scales in Dedelow (b) and Selhausen (d). For explanation of the plot layout refer to Figure 5.

465 Carry-over effects of dry and wet years towards subsequent years were also found when correlating P and SWS changes. At a two-year scale, significant correlations between P and SWS were identified to occur between 2017 and 2019 for Dedelow and from 2017 to 2019 and 2020 to 2022 for Selhausen (Fig. 6 b,i; d,i). This might be attributed to extreme wet (2017 in Dedelow) and dry conditions (2018-2020 in Dedelow and Selhausen) that were only revealed in significant correlations at scales higher than one year.

470 Note that the phase shift between the two variables at this scale from 2017 to 2019 was much larger for Selhausen (~150 days) than for Dedelow (~100 days). A reason for this could be the small Q_{net} in Dedelow 2017: during high amount of P in Dedelow very little water was drained from the lysimeter leading to greater and probably faster changes in SWS in Dedelow as compared to Selhausen. However, the patterns at the 2-year scale indicate that subsequent extreme years might lead to a carry-over effect in SWS

475 responses to P that can be derived from deviations in phase shifts in WCA spectra. Groh et al. (2020a) also observed this increased vulnerability of SWS changes in response to droughts. They found that the SWS after a drought year was not fully restored to its original value after winter when lysimeters were transferred to a site with a drier and warmer climate. Likewise, at the catchment scale Laaha et al. (2017) demonstrated that after the severe summer drought in 2015, the SWS has not been recovered. Also,

480 Boergens et al. (2020) showed that this water deficit event increased for the summer droughts from 2018 to 2019 in comparison to 2015. This might explain why the water deficit was only visible in the WCA plots at scales > 1 year after 2018 and not before.

Changing time shifts in the correlation between ET_a and SWS indicated a shift in the onset of the vegetation period towards earlier times of the year for the site under a wetter and warmer climate but not

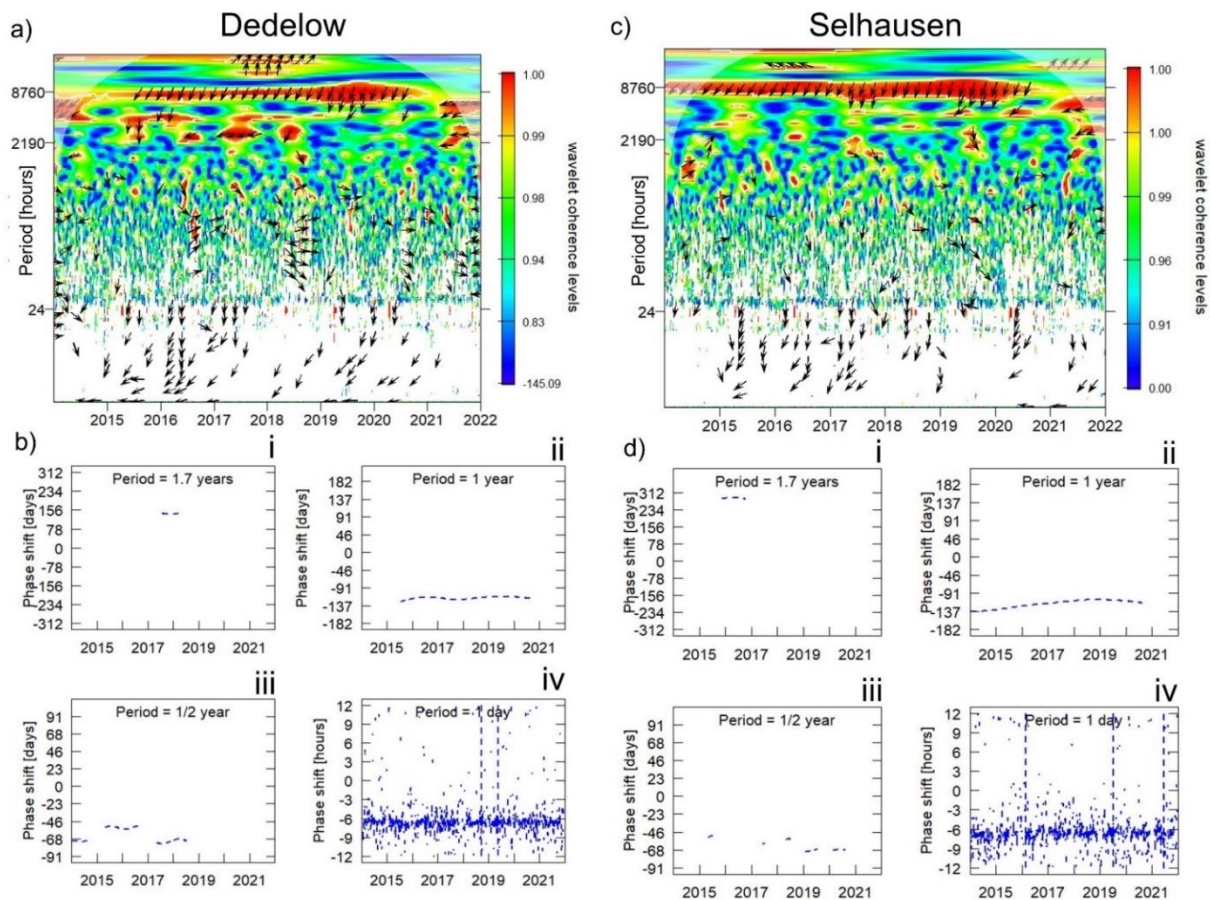
485 for the drier and colder site. A strong correlation was found between ET_a and SWS in Dedelow and Selhausen at the annual scale. The phase shift was negative indicating that ET_a was reacting in response to SWS changes (Fig. 7 a, c).

From a hydrological perspective it is interesting that ET_a and SWS are related over such a long-time scale (> 100 days, Fig. 7a, c, b ii, d ii), since ET_a should respond rather quickly to changes in the SWS. The

490 time delay in the relation between ET_a and changes in SWS at shorter times (i.e., hourly, daily) are, however, relatively stronger affected by other water balance components. Still, the time scale we are looking at is the annual scale; so, the variations observed here are more related to seasonal fluctuations

than shorter-term daily fluctuations. At a seasonal scale, the SWS starts decreasing around 90 days earlier than the ET_a (Fig. 7 b ii, d ii), which could mean that the decrease in ET_a could be buffered by taking up
495 water from deeper layers of the soil. So, the SWS will decrease but not the ET_a . This shows the importance of SWS as a variable for crop productivity.

For Dedelow the phase shift between ET_a and SWS remained constant around 120 days over the entire observation period whereas for Selhausen a decrease in temporal deviations from 136 to 90 days was observed (Fig. 7 b, ii; d, ii). This corresponded to the maximum peak in the global spectra for ET_a and
500 SWS occurring on slightly smaller scales than the annual scale (Fig. 4). Rahmati et al. (2020) found a similar trend as in Selhausen for grassland lysimeters located in two different climate regimes. They attributed the decrease in phase shift to a shift of maximum ET_a towards earlier times in the year when at the same time the maximum peak in SWS was delayed over the years. As suggested by these authors we could demonstrate that an identical phenomenon occurred in cropland. This is most likely caused due to
505 increasing temperature over the period and the earlier onset of plant decay due to drought as found by Rahmati et al. (2023). They showed that despite an earlier onset of the vegetation period the length of the growing season has been decreasing to the level of 1981 over Europe due to earlier an onset plant dormancy.



510 **Figure 7: WCA between ET_a and SWS in Dedelow (a) and Selhausen (c) and time shifts expressed in days and hours for selected scales in Dedelow (b) and Selhausen (d). For explanation of the plot layout, we refer to Figure 5.**

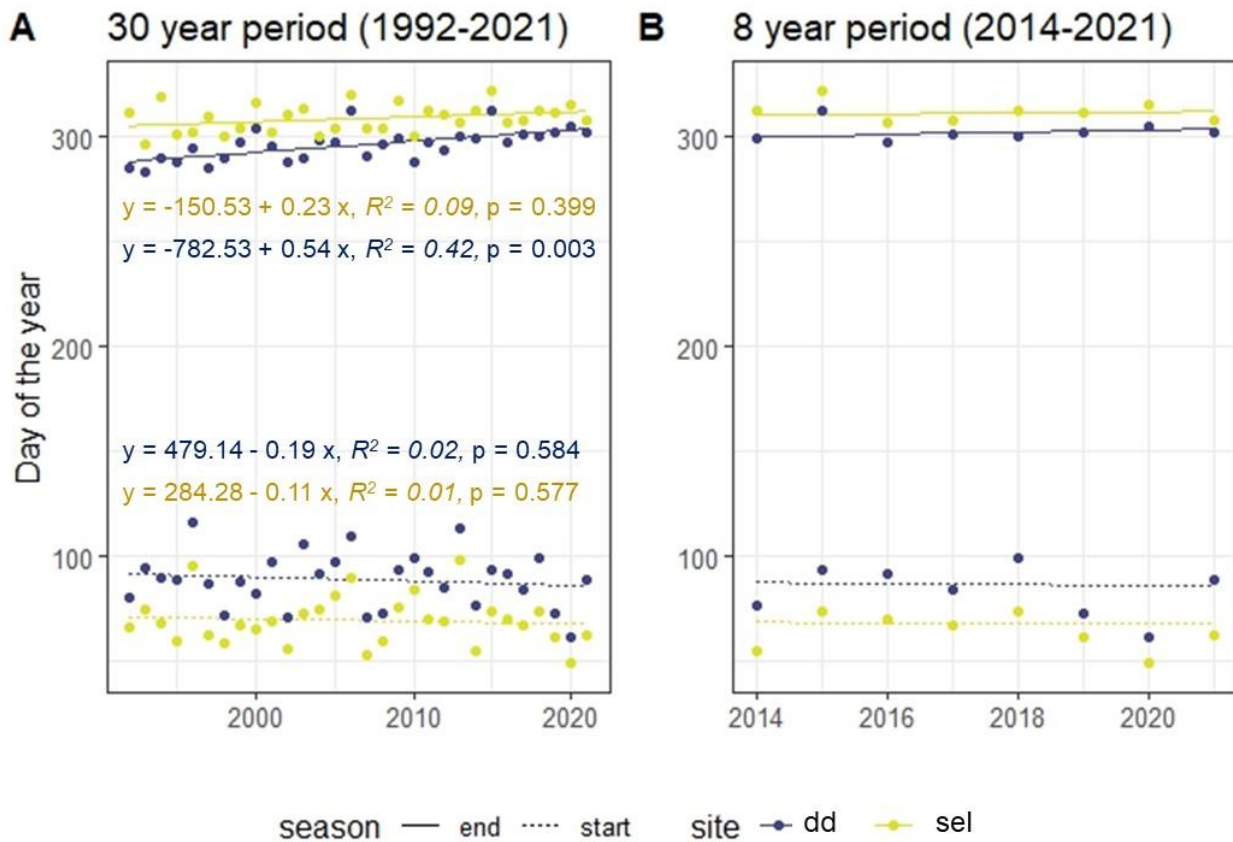
However, we did not find such a decreasing phase shift for the soil under the drier and colder climate in Dedelow at the annual scale (Fig. 7 b, ii; d, ii). The phase shift in Dedelow was about 136 days whereas in Selhausen it decreased from 136 to 90 days. One possible reason could be the differing growing season length in Dedelow and Selhausen, which influenced the amount of ET_a and SWS. For example, if the vegetation period started earlier every year at one site but not the other site, then this might explain the differences found in the WCA spectra. The length of the vegetation period at both sites was calculated from daily temperature data according to Ernst and Loeper (1976) (Fig. 8) over a thirty-year period from 1992 to 2021 and over the eight-year observation period from 2014 to 2021. The changing length of the vegetation period was calculated for the 30-year period, since the trends were more clearly visible in the longer period in comparison to the shorter eight-year period. For both periods the growing season is longer

515
520

in Selhausen in comparison to Dedelow as indicated by the earlier start and later end of the vegetation period in Selhausen. When trying to explain the different time shifts between ET_a and SWS in Selhausen and Dedelow, one needs to consider that the soils were relocated according to the space-for-time approach
525 from the drier and colder climate with the shorter growing season in Dedelow to Selhausen, where the growing season is longer and the climate warmer and wetter. Now the decreasing phase shift between ET_a and SWS that was observed for Selhausen but not for Dedelow might exactly indicate the longer growing season in Selhausen that is reflected in earlier maximum peaks of ET_a and later maximum peaks in SWS every year. The soils in Dedelow did not experience such a change since they were not subjected to
530 different climatic conditions, whereas the relocated soil had to adapt to the longer vegetation period in Selhausen. With this, an influence of changing climatic conditions on soil water budget parameters of similar soils was detectable.

Interestingly, over the last thirty years the end of the growing season is shifted stronger towards later times in Dedelow as compared to Selhausen (Fig. 8 a). However, the end of the vegetation period for
535 crops is determined by the harvest and not by the actual drop in temperatures in cropland. Therefore, the shift in the start of the growing season towards earlier times is more relevant. Thus, the difference in the end of the vegetation period cannot be used to explain the observed differences in SWS patterns between Dedelow and Selhausen.

All in all, the observed temporal changes in SWS patterns could have implications for crop production.
540 Crops will have to be planted and harvested earlier due to an earlier onset of water deficit in summer, as already suggested by some agricultural authorities (e.g., Guddat and Schwabe, 2012, Thüringer Landesanstalt für Landwirtschaft).



545 **Figure 8: Variation of beginning and end of the vegetation period in Dedelow (DD) and Selhausen (SE) over a 30-year period from 1992 to 2021 (A) and over the observation period of 8 years from 2014 to 2021 (B). Calculations were executed according to Ernst and Loeper (1976) with hourly temperature data. “End” indicates the days of each year, when the growing season stopped, whereas “start” indicates the days of each year, when growing season started.**

4 Conclusions

550 Soil water storage (SWS) dynamics are important indicators for impacts of environmental changes on the soil-water-atmosphere continuum. Temporal pattern detection and analysis of these changes might help to understand long-term impacts of droughts on plant and crop productivity.

As hypothesized, wavelet coherence analysis (WCA) of soil water balance components from lysimeters with the same soils but under different climatic conditions (drier and colder, wetter and warmer) detected
 555 differing temporal patterns with temporal shifts when correlating time series of SWS changes and actual evapotranspiration (ET_a) between both sites. Extreme wet and dry years led to a change in temporal offset in SWS changes between the two sites. In particular, years with more precipitation (P) led to a faster

response in SWS changes than years with less P, as both a lower ET_a and an earlier rewetting phase in summer and fall led to a faster reaction in the SWS changes. This shows how P affects the change in SWS
560 under different climate conditions.

The impact of droughts on SWS changes was reflected in significant periodic patterns > one year. This implies that dry years led to a carry-over effect in SWS, i.e., the SWS deficit of a dry year affected SWS of the following years. This suggests that crop production might be affected by the carry-over effect due to an earlier onset of summer drought.

565 Most interestingly, the earlier onset of vegetation periods deduced from the correlation between ET_a and SWS was only found for the site with a wetter and warmer climate and not for the site under a colder and drier climate. The soil water limitations at the drier site could be related to relatively later start of the vegetation in spring besides the cooler temperatures, and the abrupt change in climatic conditions after the transfer of the soil monoliths towards the warmer site (space-for-time substitution approach) may have
570 led to changes in the SWS. The results suggest that SWS patterns are not independent of climatic conditions. Thus, our hypothesis that there is no variation in SWS of the similarly managed arable soils at the two sites must be rejected. These results could be a first indication that a change in climatic conditions altered the soil water storage capacity. The longer term adaption of the soil water retention properties to the new climatic conditions could be a topic of future studies. The results of the present
575 study also suggest that long-term time series of SWS changes are important for understanding and quantifying environmental impact of climatic extreme events on soils and cropping systems. Limitations of the study that occur due to the co-dependency of SWS, P, ET_a , and Q_{net} should be solved by applying partial WCA in future studies.

580

Code availability

Code will be made available upon request.

Data availability

Data will be made available upon request.

585 **Authors contributions**

A. Ehrhardt: Conceptualization, Formal analysis, Investigation, Methodology, Software, Validation, Visualization, Writing – original draft preparation, Writing – review & editing

J. Groh: Conceptualization, Data curation, Formal analysis, Investigation, Methodology, Resources, Software, Writing – review & editing

590 H.H. Gerke: Conceptualization, Funding acquisition, Methodology, Project administration, Resources, Supervision, Writing – review & editing

Competing Interests

The authors declare that they have no conflict of interest.

Acknowledgements

595 The research was funded by the Leibniz Centre for Agricultural Landscape Research (ZALF), which is a research institution of the Leibniz Association in the legal form of a non-profit registered association. ZALF is financed in equal parts by the Federal Ministry of Food and Agriculture (BMEL) and the Ministry for Science, Research and Culture of the State of Brandenburg (MWFK). The study was also funded by Fachagentur Nachwachsende Rohstoffe e.V. (FNR), grant number 22404117. Jannis Groh was funded by the Deutsche Forschungsgemeinschaft (DFG, German Research Foundation) –project
600 no. 460817082. We acknowledge the support of TERENO and SOILCan, which were funded by the Helmholtz Association (HGF) and the Federal Ministry of Education and Research (BMBF). We thank Werner Küpper, Philipp Meulendick, Gernot Verch, and Jörg Haase for instrument operation and data processing at both sites.

We would like to thank Patrizia Ney from Forschungszentrum Jülich for providing the climate data for the study site Selhausen.

References

- 605 Agboma, C. and Itenfis, D.: Investigating the Spatio-Temporal dynamics in the soil water storage in Alberta's Agricultural region, *Journal of Hydrology*, 588, 125104, doi:10.1016/j.jhydrol.2020.125104, 2020.
- Allen, R. G.: Crop Evapotranspiration-Guideline for computing crop water requirements, *Irrigation and drain*, 56, 300, 1998.
- Biswas, A. and Si, B. C.: Identifying scale specific controls of soil water storage in a hummocky landscape using wavelet
610 coherency, *Geoderma*, 165, 50–59, doi:10.1016/j.geoderma.2011.07.002, 2011.
- Boeing, F., Rakovec, O., Kumar, R., Samaniego, L., Schrön, M., Hildebrandt, A., Rebmann, C., Thober, S., Müller, S., Zacharias, S., Bogena, H., Schneider, K., Kiese, R., Attinger, S., and Marx, A.: High-resolution drought simulations and comparison to soil moisture observations in Germany, *Hydrol. Earth Syst. Sci.*, 26, 5137–5161, doi:10.5194/hess-26-5137-2022, 2022.
- 615 Boergens, E., Güntner, A., Dobsław, H., and Dahle, C.: Quantifying the Central European Droughts in 2018 and 2019 With GRACE Follow-On, *Geophysical Research Letters*, 47, 179, doi:10.1029/2020GL087285, 2020.
- Bravo, S., González-Chang, M., Dec, D., Valle, S., Wendroth, O., Zúñiga, F., and Dörner, J.: Using wavelet analyses to identify temporal coherence in soil physical properties in a volcanic ash-derived soil, *Agricultural and Forest Meteorology*, 285-286, 107909, doi:10.1016/j.agrformet.2020.107909, 2020.
- 620 Büntgen, U., Urban, O., Krusic, P. J., Rybníček, M., Kolář, T., Kyncl, T., Ač, A., Koňasová, E., Čáslavský, J., Esper, J., Wagner, S., Saurer, M., Tegel, W., Dobrovolný, P., Cherubini, P., Reinig, F., and Trnka, M.: Recent European drought extremes beyond Common Era background variability, *Nat. Geosci.*, 14, 190–196, doi:10.1038/s41561-021-00698-0, 2021.
- Chen, Y., Liu, X., Ma, Y., He, J., He, Y., Zheng, C., Gao, W., and Ma, C.: Variability analysis and the conservation capacity
625 of soil water storage under different vegetation types in arid regions, *CATENA*, 230, 107269, doi:10.1016/j.catena.2023.107269, 2023.
- Ding, R., Kang, S., Vargas, R., Zhang, Y., and Hao, X.: Multiscale spectral analysis of temporal variability in evapotranspiration over irrigated cropland in an arid region, *Agricultural Water Management*, 130, 79–89, doi:10.1016/j.agwat.2013.08.019, 2013.
- 630 Ehrhardt, A., Groh, J., and Gerke, H. H.: Wavelet analysis of soil water state variables for identification of lateral subsurface flow: Lysimeter vs. field data, *Vadose zone j.*, 20, 149, doi:10.1002/vzj2.20129, 2021.
- Ernst, P. and Loeper, E. G.: *Temperaturrentwicklung und Vegetationsbeginn auf dem Grunland*, *Wirtschaftseigene Futter*, 1976.
- Farge, M.: Wavelet transforms and their applications to turbulence, *Annual review of fluid mechanics*, 24, 395–458, 1992.
- Forstner, V., Groh, J., Vremec, M., Herndl, M., Vereecken, H., Gerke, H. H., Birk, S., and Pütz, T.: Response of water fluxes
635 and biomass production to climate change in permanent grassland soil ecosystems, *Hydrol. Earth Syst. Sci.*, 25, 6087–6106, doi:10.5194/hess-25-6087-2021, 2021.

- Fu, J., Gasche, R., Wang, N., Lu, H., Butterbach-Bahl, K., and Kiese, R.: Impacts of climate and management on water balance and nitrogen leaching from montane grassland soils of S-Germany, *Environmental pollution (Barking, Essex 1987)*, 229, 119–131, doi:10.1016/j.envpol.2017.05.071, 2017.
- 640 Graf, A., Bogen, H. R., Drüe, C., Hardelauf, H., Pütz, T., Heinemann, G., and Vereecken, H.: Spatiotemporal relations between water budget components and soil water content in a forested tributary catchment, *Water Resources Research*, 50, 4837–4857, doi:10.1002/2013WR014516, 2014.
- Grinsted, A., Moore, J. C., and Jevrejeva, S.: Application of the cross wavelet transform and wavelet coherence to geophysical time series, *Nonlinear processes in geophysics*, 11, 561–566, 2004.
- 645 Groh, J., Pütz, T., Gerke, H. H., Vanderborght, J., and Vereecken, H.: Quantification and Prediction of Nighttime Evapotranspiration for Two Distinct Grassland Ecosystems, *Water Resources Research*, 55, 2961–2975, doi:10.1029/2018WR024072, 2019.
- Groh, J., Diamantopoulos, E., Duan, X., Ewert, F., Herbst, M., Holbak, M., Kamali, B., Kersebaum, K.-C., Kuhnert, M., Lischeid, G., Nendel, C., Priesack, E., Steidl, J., Sommer, M., Pütz, T., Vereecken, H., Wallor, E., Weber, T. K. D.,
650 Wegehenkel, M., Weihermüller, L., and Gerke, H. H.: Crop growth and soil water fluxes at erosion-affected arable sites: Using weighing lysimeter data for model intercomparison, *Vadose Zone Journal*, 19, e20058, 10.1002/vzj2.20058, 2020b.
- Groh, J., Diamantopoulos, E., Duan, X., Ewert, F., Heinlein, F., Herbst, M., Holbak, M., Kamali, B., Kersebaum, K.-C., Kuhnert, M., Nendel, C., Priesack, E., Steidl, J., Sommer, M., Pütz, T., Vanderborght, J., Vereecken, H., Wallor, E.,
655 Weber, T. K. D., Wegehenkel, M., Weihermüller, L., and Gerke, H. H.: Same soil, different climate: Crop model intercomparison on translocated lysimeters, *Vadose Zone Journal*, 21, 303, doi:10.1002/vzj2.20202, 2022.
- Groh, J., Slawitsch, V., Herndl, M., Graf, A., Vereecken, H., and Pütz, T.: Determining dew and hoar frost formation for a low mountain range and alpine grassland site by weighable lysimeter, *Journal of Hydrology*, 563, 372–381, doi:10.1016/j.jhydrol.2018.06.009, 2018.
- 660 Groh, J., Vanderborght, J., Pütz, T., Vogel, H.-J., Gründling, R., Rupp, H., Rahmati, M., Sommer, M., Vereecken, H., and Gerke, H. H.: Responses of soil water storage and crop water use efficiency to changing climatic conditions: a lysimeter-based space-for-time approach, *Hydrol. Earth Syst. Sci.*, 24, 1211–1225, doi:10.5194/hess-24-1211-2020, 2020a.
- Gu, X., Sun, H., Zhang, Y., Zhang, S., and Lu, C.: Partial Wavelet Coherence to Evaluate Scale-dependent Relationships
665 Between Precipitation/Surface Water and Groundwater Levels in a Groundwater System, *Water Resour Manage*, 36, 2509–2522, doi:10.1007/s11269-022-03157-6, 2022.
- Guddat, C.; Schwabe, I.: *Thüringer Pflanzenbau im Klimawandel*; Thüringer Landesanstalt für Landwirtschaft (2012): https://www.tllr.de/www/daten/agraroekologie/klima/klimawandel/pflanzenbau_klimawandel_thuringen.pdf
- He, D. and Wang, E.: On the relation between soil water holding capacity and dryland crop productivity, *Geoderma*, 353, 11–
670 24, doi:10.1016/j.geoderma.2019.06.022, 2019.

- Heistermann, M., Bogena, H., Francke, T., Güntner, A., Jakobi, J., Rasche, D., Schrön, M., Döpfer, V., Fersch, B., Groh, J., Patil, A., Pütz, T., Reich, M., Zacharias, S., Zengerle, C., and Oswald, S.: Soil moisture observation in a forested headwater catchment: combining a dense cosmic-ray neutron sensor network with roving and hydrogravimetry at the TERENO site Wüstebach, *Earth Syst. Sci. Data*, 14, 2501–2519, doi:10.5194/essd-14-2501-2022, 2022.
- 675 Herbrich, M. and Gerke, H. H.: Scales of Water Retention Dynamics Observed in Eroded Luvisols from an Arable Postglacial Soil Landscape, *Vadose Zone Journal*, 16, 1–17, doi:10.2136/vzj2017.01.0003, 2017.
- Hu, H.-M., Trouet, V., Spötl, C., Tsai, H.-C., Chien, W.-Y., Sung, W.-H., Michel, V., Yu, J.-Y., Valensi, P., Jiang, X., Duan, F., Wang, Y., Mii, H.-S., Chou, Y.-M., Lone, M. A., Wu, C.-C., Starnini, E., Zunino, M., Watanabe, T. K., Watanabe, T., Hsu, H.-H., Moore, G. W. K., Zanchetta, G., Pérez-Mejías, C., Lee, S.-Y., and Shen, C.-C.: Tracking westerly
680 wind directions over Europe since the middle Holocene, *Nature communications*, 13, 7866, doi:10.1038/s41467-022-34952-9, 2022.
- Hu, W. and Si, B.: Technical Note: Improved partial wavelet coherency for understanding scale-specific and localized bivariate relationships in geosciences, *Hydrol. Earth Syst. Sci.*, 25, 321–331, doi:10.5194/hess-25-321-2021, 2021.
- Hu, W. and Si, B. C.: Technical note: Multiple wavelet coherence for untangling scale-specific and localized multivariate
685 relationships in geosciences, *Hydrol. Earth Syst. Sci.*, 20, 3183–3191, doi:10.5194/hess-20-3183-2016, 2016.
- Hu, W., Si, B. C., Biswas, A., and Chau, H. W.: Temporally stable patterns but seasonal dependent controls of soil water content: Evidence from wavelet analyses, *Hydrological Processes*, 31, 3697–3707, doi:10.1002/hyp.11289, 2017.
- Humphrey, V. and Gudmundsson, L.: GRACE-REC: a reconstruction of climate-driven water storage changes over the last century, *Earth Syst. Sci. Data*, 11, 1153–1170, doi:10.5194/essd-11-1153-2019, 2019.
- 690 Ionita, M., Tallaksen, L. M., Kingston, D. G., Stagge, J. H., Laaha, G., van Lanen, H. A. J., Scholz, P., Chelcea, S. M., and Haslinger, K.: The European 2015 drought from a climatological perspective, *Hydrol. Earth Syst. Sci.*, 21, 1397–1419, doi:10.5194/hess-21-1397-2017, 2017.
- Jarvis, N., Groh, J., Lewan, E., Meurer, K. H. E., Durka, W., Baessler, C., Pütz, T., Ruffullayev, E., and Vereecken, H.: Coupled modelling of hydrological processes and grassland production in two contrasting climates, *Hydrol. Earth Syst. Sci.*,
695 26, 2277–2299, doi:10.5194/hess-26-2277-2022, 2022.
- Jia, X., Shao, M. 'a, Wei, X., and Wang, Y.: Hillslope scale temporal stability of soil water storage in diverse soil layers, *Journal of Hydrology*, 498, 254–264, doi:10.1016/j.jhydrol.2013.05.042, 2013.
- Kutílek, M. and Nielsen, D. R.: Soil hydrology: textbook for students of soil science, agriculture, forestry, geocology, hydrology, geomorphology and other related disciplines, Catena Verlag, 1994.
- 700 Laaha, G., Gauster, T., Tallaksen, L. M., Vidal, J.-P., Stahl, K., Prudhomme, C., Heudorfer, B., Vlnas, R., Ionita, M., van Lanen, H. A. J., Adler, M.-J., Caillouet, L., Delus, C., Fendekova, M., Gailliez, S., Hannaford, J., Kingston, D., van Loon, A. F., Mediero, L., Osuch, M., Romanowicz, R., Sauquet, E., Stagge, J. H., and Wong, W. K.: The European 2015 drought from a hydrological perspective, *Hydrol. Earth Syst. Sci.*, 21, 3001–3024, doi:10.5194/hess-21-3001-2017, 2017.

- 705 Lal, R.: Carbon Cycling in Global Drylands, *Curr Clim Change Rep*, 5, 221–232, doi:10.1007/s40641-019-00132-z, 2019.
- Lehmkuhl, F., Schüttrumpf, H., Schwarzbauer, J., Brüll, C., Dietze, M., Letmathe, P., Völker, C., and Hollert, H.: Assessment of the 2021 summer flood in Central Europe, *Environ Sci Eur*, 34, doi:10.1186/s12302-022-00685-1, 2022.
- Li, H., Sivapalan, M., Tian, F., and Liu, D.: Water and nutrient balances in a large tile-drained agricultural catchment: a distributed modeling study, *Hydrol. Earth Syst. Sci.*, 14, 2259–2275, doi:10.5194/hess-14-2259-2010, 2010.
- 710 Liu, H., Yu, Y., Zhao, W., Guo, L., Liu, J., and Yang, Q.: Inferring Subsurface Preferential Flow Features From a Wavelet Analysis of Hydrological Signals in the Shale Hills Catchment, *Water Resour. Res.*, 56, 1, doi:10.1029/2019WR026668, 2020.
- Liu, Q., Hao, Y., Stebler, E., Tanaka, N., and Zou, C. B.: Impact of Plant Functional Types on Coherence Between Precipitation and Soil Moisture: A Wavelet Analysis, *Geophys. Res. Lett.*, 44, 1, doi:10.1002/2017GL075542, 2017.
- 715 Luecke A., Puetz T., Schmidt M. (2024); TERENO data from station(s) SE_BDK_002 with parameter(s) AirHumidity, AirPressure, AirTemperature, Precipitation, WindSpeed for time period 2014-01-01 to 2021-12-31; https://hdl.handle.net/20.500.11952/TERENO.SE_BDK_002.1716629716483
- Palese, A. M., Vignozzi, N., Celano, G., Agnelli, A. E., Pagliai, M., and Xiloyannis, C.: Influence of soil management on soil physical characteristics and water storage in a mature rainfed olive orchard, *Soil and Tillage Research*, 144, 96–109, doi:10.1016/j.still.2014.07.010, 2014.
- 720 Peters, A., Groh, J., Schrader, F., Durner, W., Vereecken, H., and Pütz, T.: Towards an unbiased filter routine to determine precipitation and evapotranspiration from high precision lysimeter measurements, *Journal of Hydrology*, 549, 731–740, doi:10.1016/j.jhydrol.2017.04.015, 2017.
- Pütz, T., Kiese, R., Wollschläger, U., Groh, J., Rupp, H., Zacharias, S., Priesack, E., Gerke, H. H., Gasche, R., Bens, O., Borg, E., Baessler, C., Kaiser, K., Herbrich, M., Munch, J.-C., Sommer, M., Vogel, H.-J., Vanderborght, J., and Vereecken, H.: TERENO-SOILCan: a lysimeter-network in Germany observing soil processes and plant diversity influenced by climate change, *Environ Earth Sci*, 75, 138, doi:10.1007/s12665-016-6031-5, 2016.
- 725 Rabot, E., Wiesmeier, M., Schlüter, S., and Vogel, H.-J.: Soil structure as an indicator of soil functions: A review, *Geoderma*, 314, 122–137, doi:10.1016/j.geoderma.2017.11.009, 2018.
- 730 Rahmati, M., Groh, J., Graf, A., Pütz, T., Vanderborght, J., and Vereecken, H.: On the impact of increasing drought on the relationship between soil water content and evapotranspiration of a grassland, *Vadose zone j.*, 19, 175, doi:10.1002/vzj2.20029, 2020.
- Rahmati, M., Graf, A., Poppe Terán, C., Amelung, W., Dorigo, W., Franssen, H.-J. H., Montzka, C., Or, D., Sprenger, M., Vanderborght, J., Verhoest, N. E. C., and Vereecken, H.: Continuous increase in evaporative demand shortened the growing season of European ecosystems in the last decade, *Commun Earth Environ*, 4, doi:10.1038/s43247-023-00890-7, 2023.
- 735 Rahmstorf, S.: Is the atlantic overturning circulation approaching a tipping point?, *Oceanography*, doi:10.5670/oceanog.2024.501., 2024.

- Rieckh, H., Gerke, H. H., Siemens, J., and Sommer, M.: Water and Dissolved Carbon Fluxes in an Eroding Soil Landscape Depending on Terrain Position, *Vadose Zone Journal*, 13, 1–14, doi:10.2136/vzj2013.10.0173, 2014.
- 740 Ritter, A., Regalado, C. M., and Muñoz-Carpena, R.: Temporal Common Trends of Topsoil Water Dynamics in a Humid Subtropical Forest Watershed, *Vadose Zone Journal*, 8, 437–449, doi:10.2136/vzj2008.0054, 2009.
- Robinson, D. A., Jones, S. B., Lebron, I., Reinsch, S., Domínguez, M. T., Smith, A. R., Jones, D. L., Marshall, M. R., and Emmett, B. A.: Experimental evidence for drought induced alternative stable states of soil moisture, *Scientific reports*, 745 6, 20018, doi:10.1038/srep20018, 2016.
- Roesch, A. and Schmidbauer, H.: *WaveletComp: Computational Wavelet Analysis*, 2018.
- Schneider, J., Groh, J., Pütz, T., Helmig, R., Rothfuss, Y., Vereecken, H., and Vanderborght, J.: Prediction of soil evaporation measured with weighable lysimeters using the FAO Penman–Monteith method in combination with Richards' equation, *Vadose Zone Journal*, 20, 49, doi:10.1002/vzj2.20102, 2021.
- 750 Schnepfer, T., Groh, J., Gerke, H. H., Reichert, B., and Pütz, T.: Evaluation of precipitation measurement methods using data from a precision lysimeter network, *Hydrol. Earth Syst. Sci.*, 27, 3265–3292, doi:10.5194/hess-27-3265-2023, 2023.
- Schrader, F., Durner, W., Fank, J., Gebler, S., Pütz, T., Hannes, M., and Wollschläger, U.: Estimating Precipitation and Actual Evapotranspiration from Precision Lysimeter Measurements, *Procedia Environmental Sciences*, 19, 543–552, doi:10.1016/j.proenv.2013.06.061, 2013.
- 755 Shah, D. and Mishra, V.: Strong Influence of Changes in Terrestrial Water Storage on Flood Potential in India, *J. Geophys. Res. Atmos.*, 126, D06113, doi:10.1029/2020JD033566, 2021.
- Shen, R., Yang, H., Rinklebe, J., Bolan, N., Hu, Q., Huang, X., Wen, X., Zheng, B., and Shi, L.: Seasonal flooding wetland expansion would strongly affect soil and sediment organic carbon storage and carbon-nutrient stoichiometry, *The Science of the total environment*, 828, 154427, doi:10.1016/j.scitotenv.2022.154427, 2022.
- 760 Si, B. C.: Spatial Scaling Analyses of Soil Physical Properties: A Review of Spectral and Wavelet Methods, *Vadose Zone Journal*, 7, 547–562, doi:10.2136/vzj2007.0040, 2008.
- Si, B. C. and Zeleke, T. B.: Wavelet coherency analysis to relate saturated hydraulic properties to soil physical properties, *Water Resour. Res.*, 41, 395, doi:10.1029/2005WR004118, 2005.
- Stahl, M. O. and McColl, K. A.: The Seasonal Cycle of Surface Soil Moisture, *Journal of climate*, 35, 4997–5012, 765 doi:10.1175/JCLI-D-21-0780.1, 2022.
- Stocker, B. D., Tumber-Dávila, S. J., Konings, A. G., Anderson, M. C., Hain, C., and Jackson, R. B.: Global patterns of water storage in the rooting zones of vegetation, *Nature geoscience*, 16, 250–256, doi:10.1038/s41561-023-01125-2, 2023.
- Su, L., Miao, C., Duan, Q., Lei, X., and Li, H.: Multiple-Wavelet Coherence of World's Large Rivers With Meteorological Factors and Ocean Signals, *JGR Atmospheres*, 124, 4932–4954, doi:10.1029/2018JD029842, 2019.
- 770 Tafasca, S., Ducharne, A., and Valentin, C.: Weak sensitivity of the terrestrial water budget to global soil texture maps in the ORCHIDEE land surface model, *Hydrol. Earth Syst. Sci.*, 24, 3753–3774, doi:10.5194/hess-24-3753-2020, 2020.
- Torrence, C. and Compo, G. P.: A practical guide to wavelet analysis, *B. Am. Meteorol. Soc.*, 79, 61–78, 1998.

- Torrence, C. and Webster, P. J.: Interdecadal changes in the ENSO–monsoon system, *Journal of climate*, 12, 2679–2690, 1999.
- 775 Trautmann, T., Koirala, S., Carvalhais, N., Güntner, A., and Jung, M.: The importance of vegetation in understanding terrestrial water storage variations, *Hydrol. Earth Syst. Sci.*, 26, 1089–1109, doi:10.5194/hess-26-1089-2022, 2022.
- Vereecken, H., Pachepsky, Y., Simmer, C., Rihani, J., Kunothe, A., Korres, W., Graf, A., Franssen, H.J.-H., Thiele-Eich, I., and Shao, Y.: On the role of patterns in understanding the functioning of soil-vegetation-atmosphere systems, *Journal of Hydrology*, 542, 63–86, doi:10.1016/j.jhydrol.2016.08.053, 2016.
- 780 Vereecken, H., Amelung, W., Bauke, S. L., Bogena, H., Brüggemann, N., Montzka, C., Vanderborght, J., Bechtold, M., Blöschl, G., and Carminati, A.: Soil hydrology in the Earth system, *Nature Reviews Earth & Environment*, 3, 573–587, 2022.
- Yang, Y., Wendroth, O., and Walton, R. J.: Temporal Dynamics and Stability of Spatial Soil Matric Potential in Two Land Use Systems, *Vadose zone j.*, 15, 1–15, doi:10.2136/vzj2015.12.0157, 2016.
- 785 Yu, M., Zhang, L., Xu, X., Feger, K.-H., Wang, Y., Liu, W., and Schwärzel, K.: Impact of land-use changes on soil hydraulic properties of Calcaric Regosols on the Loess Plateau, NW China, *J. Plant Nutr. Soil Sci.*, 178, 486–498, doi:10.1002/jpln.201400090, 2015.

Appendix

Table A1: Annual precipitation, actual evapotranspiration (ET_a), drainage, upward water flow and change in soil water storage (SWS) for Dedelow (Dd) and Selhausen (Sel) calculated from the lysimeter weights.

790 Data are given in mm a^{-1} .

	Precipitation [mm a^{-1}]		ET_a [mm a^{-1}]		Drainage [mm a^{-1}]		Upward Flow [mm a^{-1}]		Δ SWS [mm a^{-1}]	
	Dd	Sel	Dd	Sel	Dd	Sel	Dd	Sel	Dd	Sel
2014	676	873	579	676	21	314	-36	-38	111	-79
2015	542	744	619	691	78	125	-70	-87	-85	15
2016	534	702	556	464	28	271	-60	-48	10	16
2017	872	642	700	601	167	96	-42	-68	46	13
2018	400	534	474	526	109	131	-82	-77	-100	-47
2019	575	673	572	543	3	155	-52	-62	52	37
2020	498	581	503	475	26	172	-31	-40	0	-26
2021	757	768	507	571	188	157	-12	-61	74	100
Sum	4854	5517	4510	4547	620	1421	-385	-481	108	29
Mean	607	690	564	568	78	178	-48	-60	14	4

Global wavelet spectra Qnet DD vs. Sel

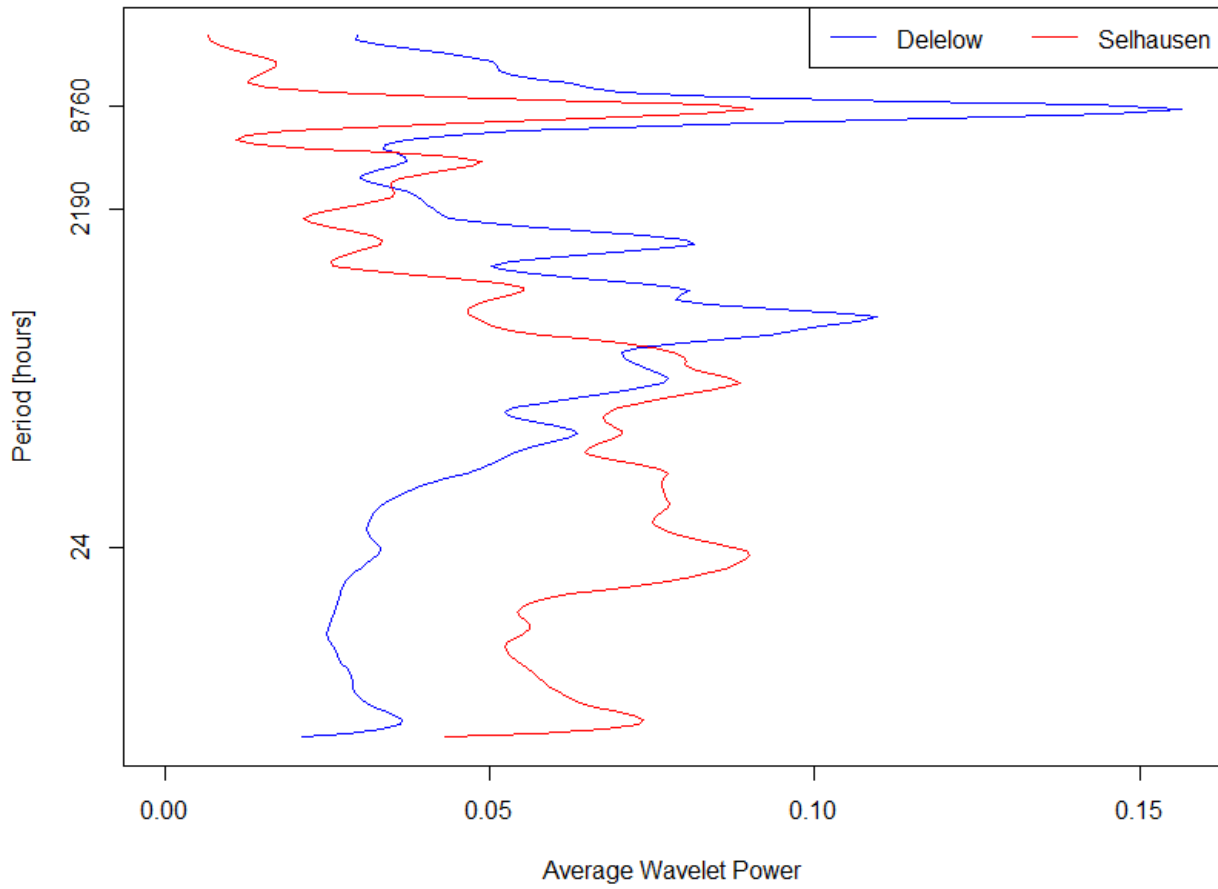


Figure B1: Periods (hours) versus average wavelet power of the global wavelet spectra for Q_{net} from Dedelow and Selhausen.

795

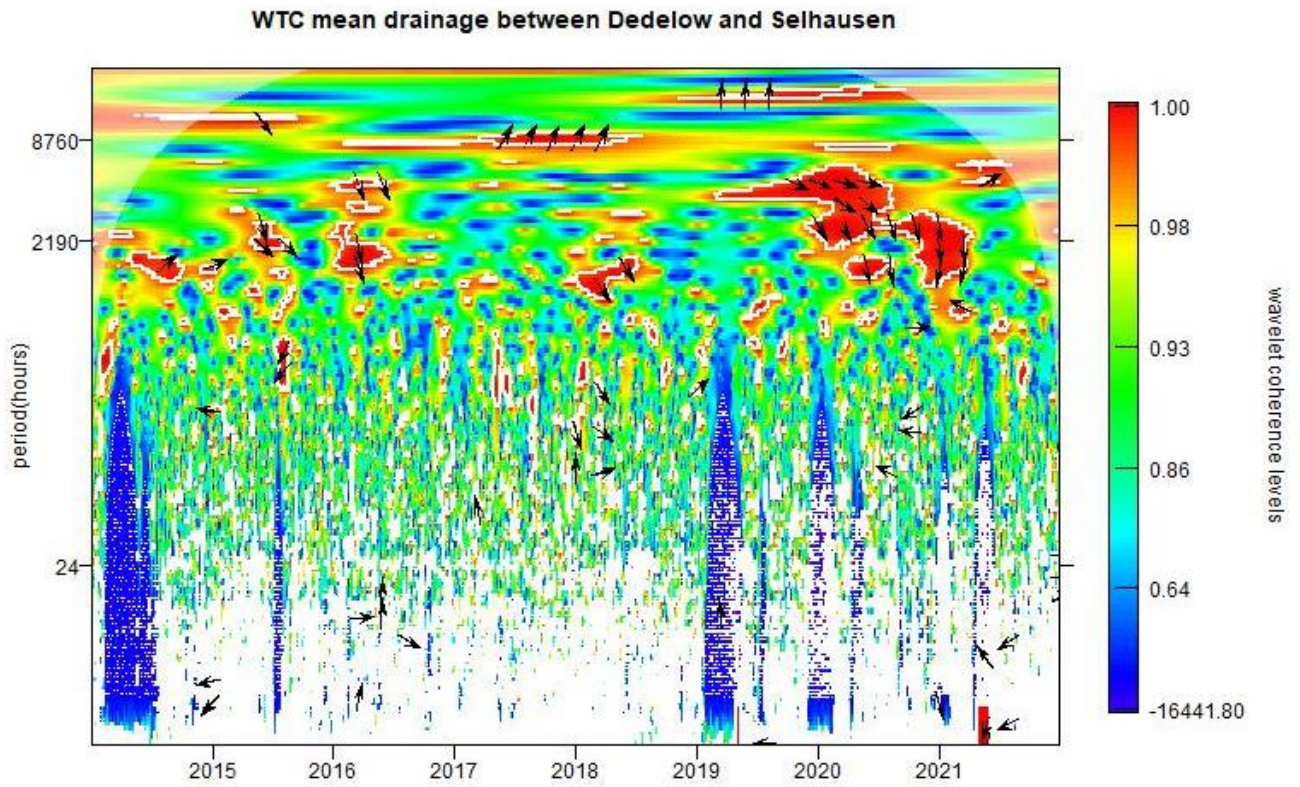


Figure C1: Wavelet coherency spectrum of Q_{net} in Dedelow and Selhausen

800

WTC between Drainage and mean SWS in Dedelow

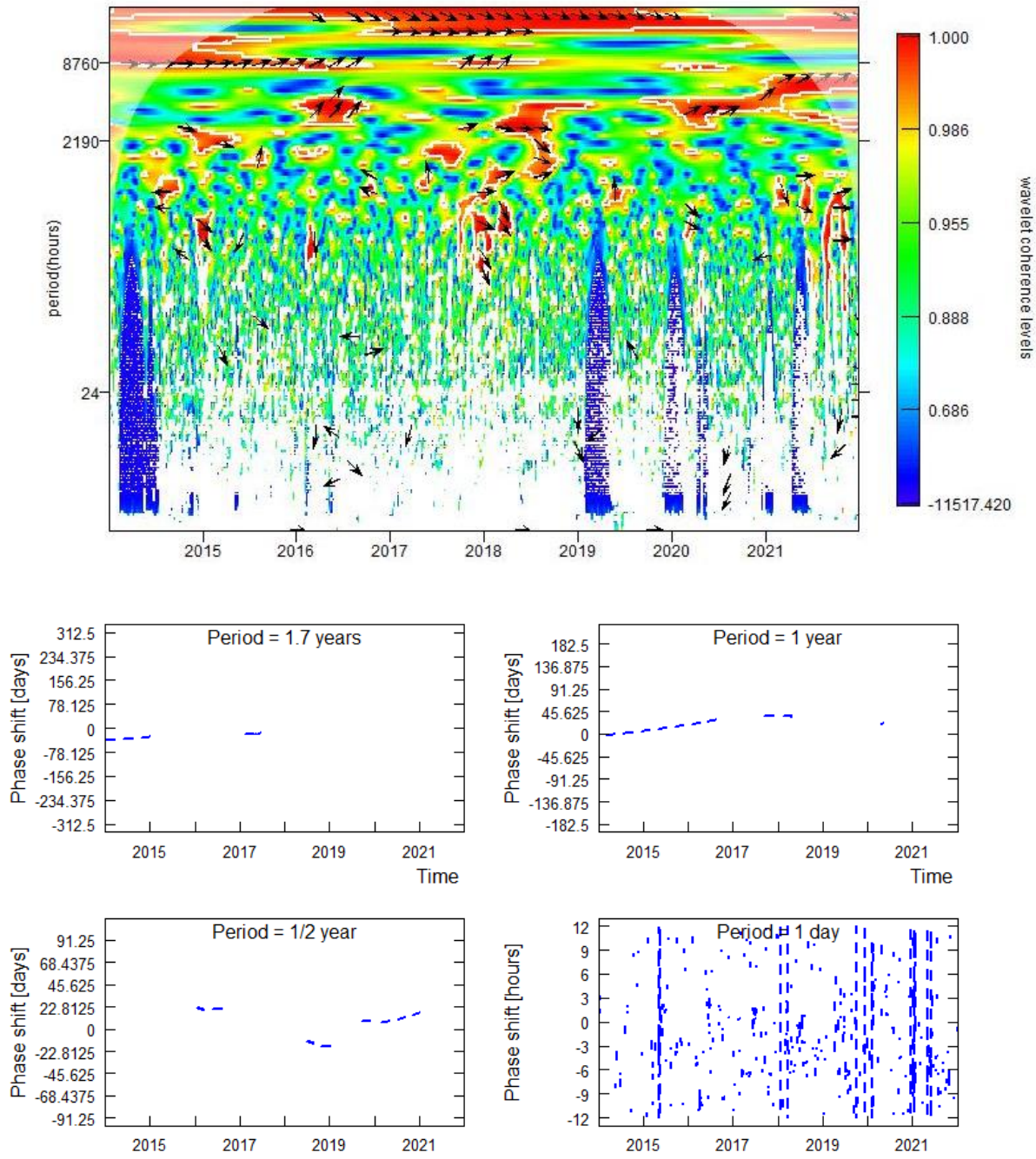


Figure C2: Wavelet coherency spectrum and time shifts between Q_{net} and SWS in Dedelow

WTC between Drainage and mean SWS in Selhausen

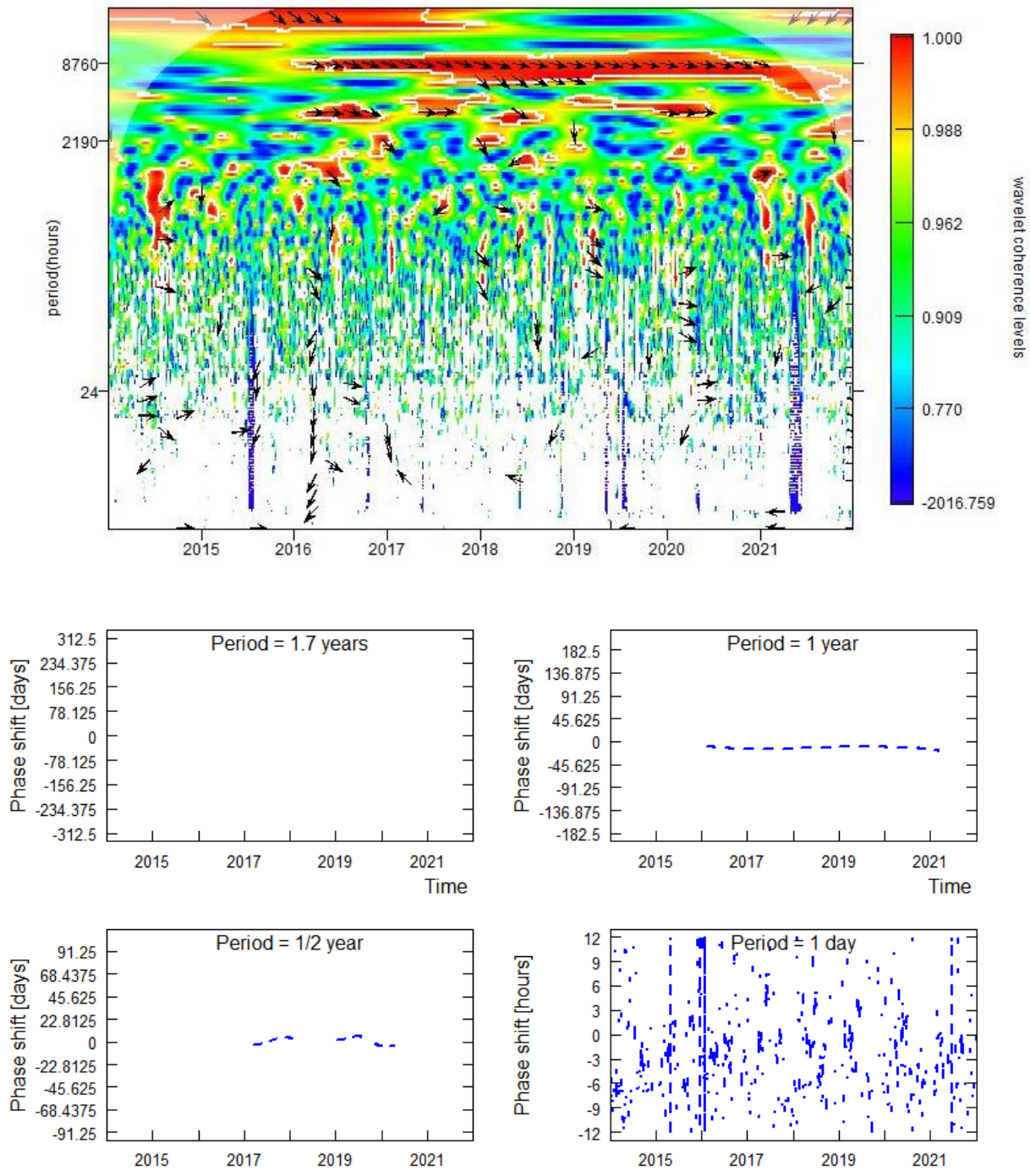


Figure C3: Wavelet coherence spectrum and time shifts between Q_{net} and SWS in Selhausen